



Palaeoseismological assessment for a seismic gap located very close to the epicentre of the 30 October 2020 Samos Earthquake ($M_6.9$), western Anatolia, Turkey

Umut Öncü¹ · Hasan Sözbilir^{2,3} · Çağlar Özkaymak^{4,5} · Mustafa Softa^{2,3} ·
Ökmen Sümer² · Semih Eski^{1,2} · Joel Q. G. Spencer⁶ · Eren Şahiner⁷ ·
Mehmet Yüksel⁸ · Niyazi Meriç⁷ · Mustafa Topaksu⁸

Received: 17 March 2023 / Accepted: 26 October 2023 / Published online: 25 January 2024
© The Author(s) 2023

Abstract

The Tuzla Fault (TF), considered one of the most important seismic sources in İzmir province, is defined as a strike–slip fault with N10E–N60E striking between Gaziemir and Doğanbey districts. A 50-km-long fault consists of three segments which are, from north to south Çatalca, Orhanlı, and Doğanbey segments. Recent studies claim that the part of the TF extending to Kuşadası Bay is also in a kinematic relationship with the Samos Fault that caused an earthquake on 30 October 2020 ($M_w = 6.9$). In this study, in order to analyse the historical behaviour of the fault, three trench-based palaeoseismology studies across the fault scarp were conducted on three geometric segments of the TF. Palaeoseismology findings show that seven historic/prehistoric earthquakes were generated by TF. According to Oxcal distribution using the Bayesian methods, the time of the events lie between 46.2 ± 6.1 and 1.6 ± 0.3 ka. When the events are compared with the historical earthquakes, the last event is correlated with the earthquakes of 47 AD and/or 177/178 AD on the Doğanbey segment. Moreover, the other events can be attributed to the late Pleistocene–Holocene earthquakes that are prehistorical periods. Our results provide a recurrence interval of an earthquake along the TF to between 0.7 and 4.3 ka for the Holocene period. The elapsed time since the most recent surface faulting earthquake on the TF is 1844 years. It is suggested that it is predicted that TF has the potential to produce destructive earthquakes in the near future, especially in Orhanlı and Çatalca segments which may be considered as a seismic gap.

Keywords Tuzla Fault · Palaeoseismology · Seismic hazard · Earthquakes · Western Anatolia

Abbreviations

TF	Tuzla Fault
GF	Gülbağçe Fault
YF	Yağcılar Fault
NAFZ	North Anatolian Fault Zone
EAFZ	East Anatolian Fault Zone

Extended author information available on the last page of the article

İBTZ	İZmir-Balıkesir Transfer Zone
OSL	Optically stimulated luminescence
TL	Thermoluminescence
SAR	Single aliquot regenerative dose
D_e	Equivalent dose
MAM	Minimum Age Model
CAM	Central age model
DEM	Digital elevation model
AD	Anno Domini
BC	Before Christ

1 Introduction

Large earthquakes are well-known natural hazard phenomena occurring at known, undefined, or underestimated seismic sources. There are a quite number of devastating earthquakes that have underestimated seismic sources globally such as the 2008 Wenchuan (China) and the 2011 Van (Turkey) earthquakes, with over 80 and 1 k fatalities, respectively (e.g. Mackenzie et al. 2016; Chen et al. 2018; Fan et al. 2018). From this point of view, it is vital to shed light on active seismic sources and their earthquake recurrence interval, slip rates, and the elapsed time since the most recent earthquake in order to mitigate such hazards and their detrimental effects.

Palaeoseismology studies are the most common mitigation techniques for understanding earthquake potential for seismic sources since the final decade of the 1800's (Galli et al. 2008; Jayangondaperumal et al. 2018). However, palaeoseismological, seismological, geomorphological, and geodesy studies are also used as eminent tools to estimate seismic hazard parameters of the regions and/or faults (e.g. Campbell 1982; Rockwell et al. 1984; Bürgmann et al. 1997; Silva et al. 2003; Reilinger et al. 2006, 2010; Aktuğ et al. 2013, 2021; Priyanka et al. 2017; Akkar et al. 2018).

Globally between 1986 and 2022 over 1 k studies report palaeoseismological investigations (Softa and Utku 2022). From these studies, the first palaeoearthquake records of mainly strike–slip faults were initiated on the segments of the North Anatolian Fault Zone (NAFZ) (Turkey) in the early 1990s (e.g. Ikeda et al. 1991). After the 1999-Kocaeli and Düzce earthquakes (Mw:7.4 and 7.2, respectively), palaeoseismology studies, a significant part of which were carried out on the NAFZ, were later applied on the East Anatolian Fault Zone (EAFZ) and the reverse fault-dominated Eastern Anatolia Fault due to the 2011 Van earthquake (e.g. Gürboğa and Gökçe, 2019).

Similarly, the first palaeoseismology study on normal faults in western Anatolia was carried out by Altunel et al. (1999) after the 1995 Dinar earthquake. Recently, palaeoseismology studies on the Sultandağı Fault (Akyüz et al. 2006), Manisa Fault (Özkaymak et al. 2011; Akçar et al. 2012; Mozafari et al. 2021; Duran et al. 2021; Softa et al. 2023), Yatağan Fault (Akyüz et al. 2019; Basmenji et al. 2021), Muğla Fault (Karabacak 2016), Milas Fault (Akyüz et al. 2019; Kırkan et al. 2019, 2023), and Gökova Fault (Dikbaş et al. 2022) have shown that normal faults in the western Anatolia have low slip rates with long-term earthquake recurrence periods.

While the faults in western Anatolia may pose a lower threat compared to the NAFZ, which exhibits strike-slip characteristics, the western Anatolia area experiences distributed seismic activity that is more challenging to predict accurately than regional faults like

NAFZ and EAFZ. The İzmir-Balıkesir Fault Zone (İBTZ) is believed to play a significant role in accommodating differential extensional strain within the Aegean Extensional System (e.g. Uzel and Sözbilir 2008; Özkaymak et al. 2011; 2013). The İBTZ NE-trending transfer zone includes a number of secondary strike–slip faults such as the Tuzla, Gülbahçe, Seferihisar and Yağcılar Faults and normal faults such as the İzmir Fault, Manisa Fault, Kemalpaşa and Gümüldür Fault, which are striking NE–SE/NW–SE and approximately E–W, respectively (e.g. Emre et al. 2005; Uzel and Sözbilir 2008; Özkaymak et al. 2011, 2013; Uzel et al. 2015).

As mentioned, the Tuzla Fault (TF), Yağcılar Fault, and Gülbahçe Fault are active segments within the İBTZ. Despite research by many scientists on the kinematic properties, seismicity, and geothermal energy potential of these three faults, they have not been extensively investigated, except for the palaeoseismology studies of Şengöçmen Geçkin et al. (2022) on the Gülbahçe Fault. Besides this, the fault trace of the TF terminates to the south-west on land and it lies ~ 15 km from the epicentre of the 2020 Samos earthquake (Mw: 6.9) (Figs. 1 and 2). Soon after the main shock, seismic flocculation and hot water outflow on the SE edge of TF (Aktuğ et al. 2021; Uzelli et al. 2021; Şengöçmen Geçkin et al. 2022) indicate stress transfer on the hanging wall of the Samos Fault where the TF is located.

To unravel Quaternary earthquake activity and surface rupture events, we aimed to study seismotectonic behaviour of the TF by conducting trench-based palaeoseismological surveys to reveal (i) Holocene and Pleistocene earthquake activity, (ii) average recurrence interval, and (iii) elapsed time since the last earthquake by using optically stimulated luminescence (OSL) dating methods. This study reveals the earthquake history of TF and provides prominent datasets that can be used for earthquake hazard mitigation assessment between İzmir-Doğanbey and İzmir-Gaziemir province.

2 Regional geology and seismotectonic setting

Western Anatolia, which has been shaped under the effect of N-S directed continental extension since the Pliocene, has a complex structure that progresses to the south-west under the control of the Aegean/Cyprus arc where the African oceanic lithosphere subducts under the Anatolian plate (Fig. 1).

The Anatolian Plate moving westward, presents different deformation patterns in the eastern, central, and western sections. The deformation level formed in the region with high seismicity along the plate boundaries is the source of many intracontinental faults. While fault segments with relatively high slip rates are observed on the North and the East Anatolian fault system (Şengör et al. 2005; Duman and Emre 2013; Tatar et al. 2020), The Central Anatolian “ova” region contains fault segments with lower slip rate values (Şengör et al. 1985; Kürçer and Gökten 2014).

The westward movement of the Anatolian Plate along the North Anatolian Fault and East Anatolian Fault changes direction to increase towards the south-west when it enters the NE–SW-trending İBTZ where both normal and strike–slip faults correspond to the current deformation. The TF forms the eastern boundary of the southern part of the İBTZ on a regional scale and limits the Seferihisar High from the east. It is stated that the TF, whose important parts extend inland, also continues in the sea (Oçakoğlu et al. 2004, 2005; Gürçay 2014). It is accepted that the TF produced destructive earthquakes that shaped the

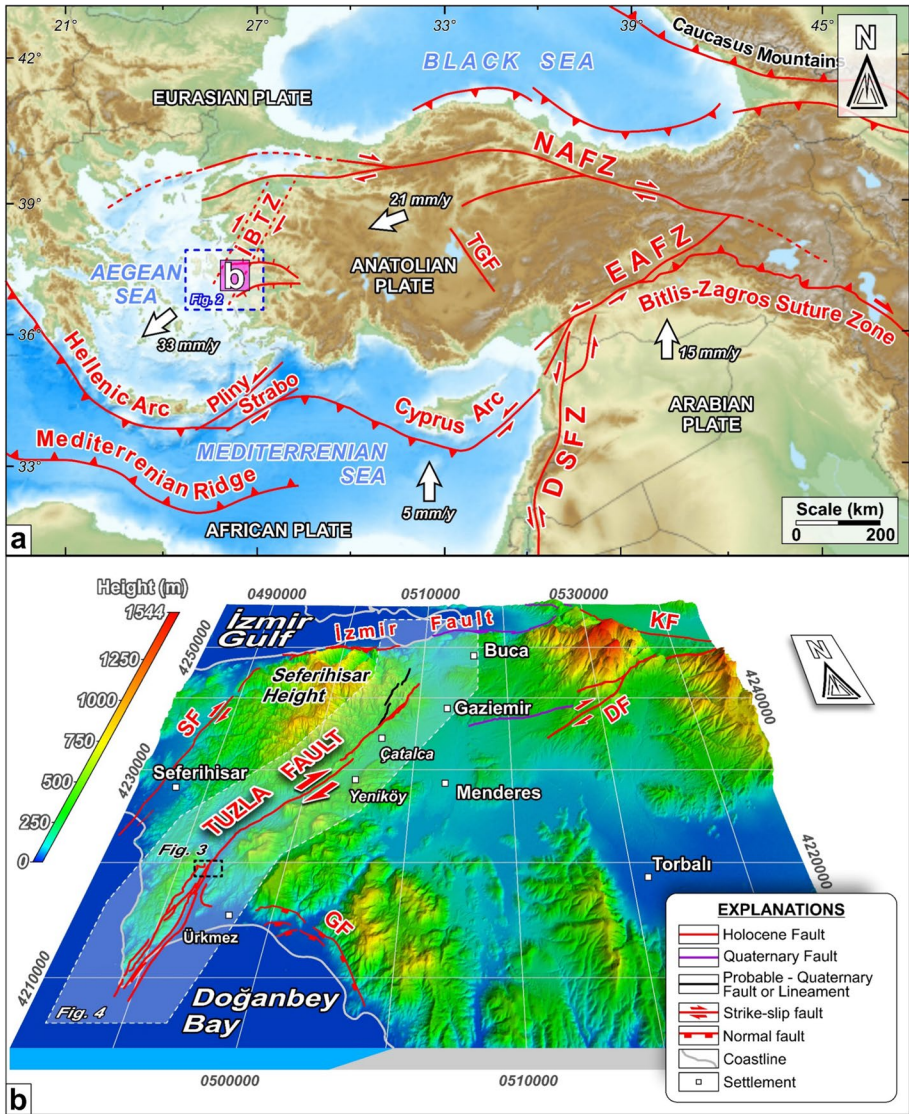


Fig. 1 Location map of the study area (a) Regional tectonic structure map of Turkey and its surroundings (Barka 1992, 1999; Uzel and Sözbilir 2008; Uzel et al. 2013; Meng et al. 2021). The number beside each white arrow indicates the slip rate of plates from GPS data in mm/y (Reilinger et al. 2006). (b) Main parts of the Tuzla Fault and its surroundings; 3D DEM map showing structural elements (Emre and Özalp 2011; Emre et al. 2011). NAFZ North Anatolian Fault Zone; EAFZ East Anatolian Fault Zone; DSFZ Dead Sea Fault Zone; İBTZ İzmir-Balıkesir Transfer Zone; TGF Tuz Gölü Fault; SF Seferihisar Fault; KF Kemalpaşa Fault; DF Dağkızılcıca Fault; GF Gümüldür Fault

tectonic structure in the region, resulting in surface faulting in the Holocene period, and therefore, it is an important seismic source for the province of İzmir in the future.

The seismotectonics of the region is controlled by the westward extrusion of the Anatolian plate, between Arabian, Eurasian and African plates as a result of processes between

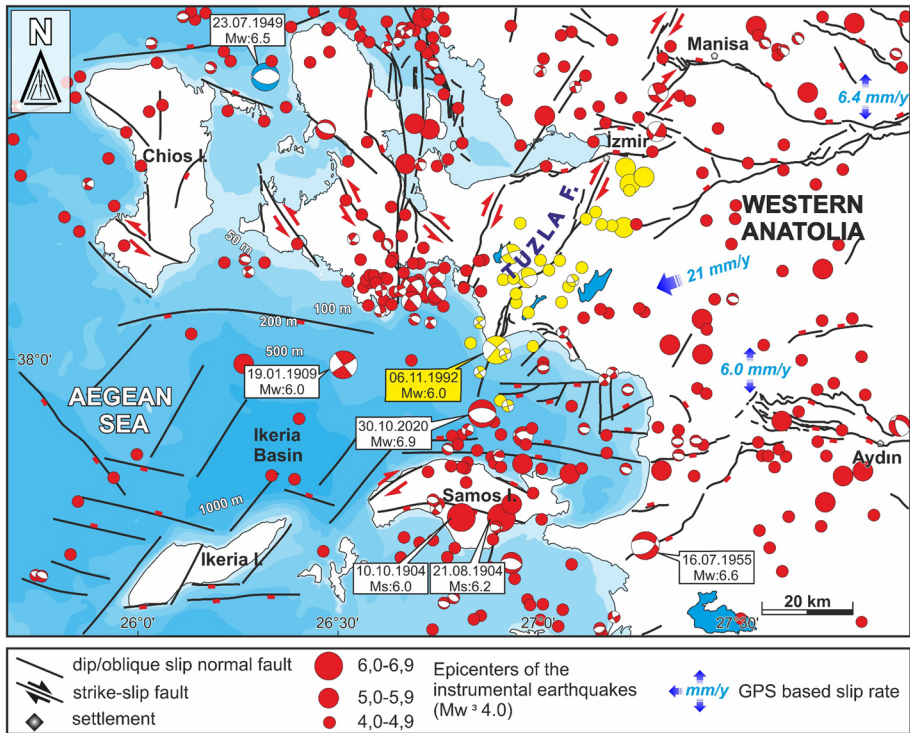


Fig. 2 Seismotectonic map of the İzmir and nearby area (Aktuğ et al. 2021; While the instrumental seismicity between 1900 and 2023 are compiled from ISC, 2023, faults are compiled from Lykousis et al. 1995; Ocakoğlu et al. 2004; Pavlides et al. 2009; Caputo and Pavlides 2013; Emre et al. 2018)

them such as collision, subduction, back-arc spreading, and slab tearing (Şengör et al. 1985; Armijo et al. 1999; Reilinger et al. 2006; Jolivet et al. 2013). The westward relative motion causes an internal deformation along the borders of tectonic blocks in western Anatolia (i.e. Sözbilir et al. 2003, 2011; Nyst and Thatcher 2004; Reilinger et al. 2006; Aktuğ et al. 2009; Emre et al. 2018). In general, ~E–W-trending active normal faults and NE–SW-trending active strike–slip faults bounding these tectonic blocks play an important role in seismicity of the region (Sözbilir et al. 2003, 2011; Emre et al. 2005, 2011, 2018; Özkaymak and Sözbilir 2008, 2012; Uzel and Sözbilir 2008; Akçar et al. 2012; Özkaymak et al. 2013; Duman et al. 2018; Eyübagil et al. 2021; Mozafari et al. 2021, 2022).

According to the historical earthquake catalogue of İzmir city and nearby area, 33 historical earthquakes were recorded after 47 AD and 17 earthquakes with intensity of VII and greater (Table 1) (Ergin et al. 1967; Soysal et al. 1981; Guidoboni et al. 1994; Ambraseys and Finkel 1995; Ambraseys and Jackson 1998; Tan et al. 2008; Başarıır Baştürk et al. 2016; Tepe et al. 2021). Most of them were recorded in İzmir, formally the ancient city of Smyrna, the biggest city in western Anatolia, and the source of most of them are not yet known except for the 178, 1688, and 1778 AD events which were suggested to be related with the segments of the E–W-trending İzmir Fault (Sözbilir et al. 2021; Tepe et al. 2021).

During the instrumental period, about 30 earthquakes have been reported on the TF and nearby areas with a magnitude of 4.0 and greater (Fig. 2). The most damaging of these

Table 1 List of recorded historical earthquakes in the İzmir and surrounding area

ID No	Time	Location	Coordinates		Intensity	References
			Lat	Long		
60	47 AD	İzmir region			VIII	NA EG NB
			38.45	27.18		
100	178 AD	İzmir				HS
	177 AD	İzmir, Miletus, Chios, Samos	38.40	27.10	X	HS
	178 AD	İzmir			X	EG
250	688 AD	İzmir	38.40	27.00	IX	HS
324	1040, Feb. 2 AD	İzmir	38.40	27.15	VII	HS
335	1056 AD	İzmir region	38.40	27.15	VIII	HS
499	1463 AD	Aegean Sea				NA NB
			38.41	27.12		
676	1654 AD	İzmir				NA HS
			38.40	27.20	VI	
689	1664, June 2 AD	İzmir				NA HS
			38.41	27.20	VII	
695	1667, Nov. AD	İzmir				AF HS
	1667 AD		38.40	27.20	VII	
727	1682, July 16 AD	İzmir				NA NB
			38.41	27.12	VIII	
735	1687, Nov. 11 AD	İzmir				NA HS
	1687, Dec. 18 AD		38.40	27.20	VI	
737	1688, July 10 AD	İzmir				NA HS
			38.40	27.20	X	
739	1688, July 11 AD	İzmir			VI	HS NB
			38.41	27.12		
808	1717, July 1 AD	İzmir				NA HS
			38.40	27.10	V	
827	1723, Sep. AD	İzmir				NA NB
			38.41	27.12		
858	1739, May 1 AD	İzmir	38.40	27.20	VI	HS
868	1745, Mar. 18 AD	İzmir	38.41	27.12		NB
894	1754, July AD	İzmir				NA HS
			38.40	27.15	VII	
1005	1771, Aug. 8 AD	İzmir	38.40	27.20	VI	HS
1020	1776, June 16 AD	İzmir	38.40	27.20	VIII	HS
1029	1778, July 3 AD	İzmir				NA HS
			38.40	27.20	VIII	
1032	1778, Oct. 1 AD	İzmir				NA HS
			38.40	27.20	VIII	
1057	1785, Apr. 26 AD	İzmir	38.40	27.15	VI	HS
1176	1828, June 15 AD	İzmir				NA HS
			38,4	27.20	VII	
			38.41	27.13	VII	STU

Table 1 (continued)

ID No	Time	Location	Coordinates		Intensity	References
			Lat	Long		
1180	1829, Feb. 23 AD	İzmir				NA
			38.40	27.20	VI	HS
1235	1839, Oct. 22 AD	İzmir	38.40	27.15	VI	HS
1254	1841, Nov. 27 AD	İzmir	38.40	27.20	VII	HS
1405	1852, Sep. 8 AD	İzmir				NA
			38.41	27.12	V	NB
1462	1855, Dec. 18 AD	İzmir	38.40	27.20	VII	NA
						HS
1486	1857, Feb. 13 AD	İzmir				NA
	1857, Feb. 12 AD		38.40	27.20	VII	HS
1635	1866, Apr. 25 AD	Samos Island, Aegean Sea	38.40	27.20	VI	NA
						HS
2213	1899, Jan. 21 AD	Menderes, İzmir	38.24	27.13	V	NA
						NB
2215	1899, Jan. 27 AD	Menderes, İzmir	38.24	27.13		NA
						NB

References: (EG) Guidoboni et al. (1994); (HS) Soysal et al. (1981); (NA) Ambraseys (2009); (STU) Stucchi et al. (2012); (NB) Başarır Baştürk et al. (2016). Abbreviations: *BC* Before Christ; *AD* Anno domini

occurred on 6 November 1992 (Mw: 6.0) with an epicentre at the most southern part of the TF (the Doğanbey segment) in the Aegean Sea, causing severe damage in the villages around the city of İzmir, but it did not produce any surface deformations on land (Scordilis et al. 1994; Tan et al. 2008). Focal mechanism solutions of 1992 (Mw: 6.0) and another 7 earthquakes (Mw: 4.0–5.8) indicate the existence of a right-lateral strike–slip faulting sense with the NE–SW-trending TF (Fig. 2). According to Scordilis et al. (1994), the mainshock of the 1992 earthquake occurred on a 16-km-long fault segment; the focal depth was 9 km (aftershocks ranged from 5 to 13 km depth) and the rupture propagated towards the NNE. Some moderate earthquakes were also reported on or around the TF on 23 November 1902 (Mw: 5.5), 19 May 1904 (Mw: 5.4), 16 December 1977 (Mw: 5.5), and 17 April 2003 (Mw: 5.2).

It is accepted that the last destructive earthquake on the TF, which is considered as one of the important seismic sources in the İzmir province, occurred on 6 November 1992 (Seferihisar Bay earthquake, Ms: 6.0) on the extension of the Doğanbey segment into the sea (Türkelli et al. 1995; Tan and Taymaz 2001, 2003). In addition, the Samos earthquake that occurred on 30 October 2020 caused 117 fatalities and many collapsed and severely damaged buildings in the İzmir/Bayraklı district. Our results indicate that the segment of the TF extending to Kuşadası Bay is in a kinematic relationship with the Samos Fault.

3 Methods

3.1 Field survey

In this study, we used 1/25000 scale topographic maps acquired from the General Directorate of Mineral Research and Exploration (Turkey), aerial photos, ALOS PALSAR-12.5 m DEM, and Google Earth imagery, and these were combined with detailed field surveys to map the fault traces to locate suitable sites for trenching. Suitable sites were selected based on fault morphology and where the young sediments are as stratigraphically continuous as possible.

3.2 Palaeoseismology

In order to better understand the palaeoearthquake evidence along the TF, we conducted trench investigations at the Çatalca site on the Çatalca segment, at the Yeniköy site on the Orhanlı segment, and at the Tuzla site on the Doğanbey segment. Here, we focus on the excavation, description, and sampling of the trenches. Each trench was up to 24 m long and 3.5 m deep. The width of the trenches was 3 m. Following McCalpin (2009), we assigned the exposed units numbers and they were described based on their microstratigraphic position. During the trench studies, after cleaning of the trench walls, they were gridded with horizontal and vertical strings with 1 m spacing. Then, sedimentary boundaries and structural features were mapped in detail with a scale of 1/20 using graph paper, and all sections photographed. Lastly, samples were collected for optically stimulated luminescence (OSL) dating of quartz minerals from event horizons. OSL is one of the best known and most suitable dating techniques for determination of deposition age of late Quaternary sediments (e.g. Preusser et al. 2008; Rhodes 2011; Mahan et al. 2022). In particular, OSL dating has enabled the direct dating of the wedge, colluvium, and recent deposits (e.g. Spencer et al. 2003, 2019; Fattahi et al. 2006, 2010; Doğan et al. 2015; Softa et al. 2021; Softa and Utku 2022) and has been applied successfully to palaeoseismology studies in the world (e.g. Lee et al. 2001; Prentice et al. 2002; Bookhagen et al. 2006; Rittase et al. 2014; Stahl et al. 2016; Tsodoulos et al. 2016; Jayangondaperumal et al. 2017; Duran et al. 2021). For this reason, OSL dating was chosen to constrain the timing of identified earthquake surface faulting events.

Seventeen samples were collected from the trench walls using 52×150 mm metal cylinders, taking care to limit any light contact on the open cylinder ends and assuring that sediments filled the cylinder to avoid inadvertent mixing of any light-exposed grains at the cylinder ends. As an additional precaution, sampling was undertaken during a moonless night. The samples were processed at the Dokuz Eylül University (DEU) sample preparation laboratory for luminescence dating and the mineral separation steps to extract quartz from the sediments required for age determination were completed according to the standard procedures described by Aitken (1998) and Spencer and Robinson (2008). The following procedures were performed for equivalent dose and dose rate measurement at the Institute of Nuclear Science in Ankara University and the TL/OSL Dating Laboratory at Çukurova University Arts-Sciences Faculty Physics Department. The OSL ages were calculated by dividing the OSL equivalent dose measurement by the total dose rate, according to Aitken (1998). After gathering robust OSL data that have satisfied a variety of data quality tests, all the luminescence ages were refined by Bayesian methods in OxCal with

respect to historical earthquakes. Bayesian analysis uses a likelihood statistical approach that evaluates information such as laboratory uncertainties and stratigraphic relationships, to determine posterior distributions of the original age determinations. Using this OxCal model, the data are constructed as a simple sequence (Ramsey 1995, 2001) with all luminescence ages plotted with 2σ uncertainties and 95% confidence ranges.

The OSL method determines the time elapsed since the last daylight exposure of mineral grains within each sedimentary unit sampled in the trench walls. In order to measure the equivalent dose, the single-aliquot regenerative dose (SAR) protocol (Murray and Wintle 2000) was applied to all samples. In the first part of each measurement cycle, a preheat of 220 °C for 10 s was used to remove charge from thermally unstable traps subsequent to natural or regenerative dose, before measurement of the OSL signal. Any change in luminescence sensitivity was monitored, and corrected for, in the second part of the cycle by administering a constant test dose of 5 Gy followed by a cutheat of 160 °C before OSL measurement of the test dose signal. OSL measurements were performed with a sample temperature of 125 °C using constant power blue LEDs (80% optical power) for a stimulation time of 120 s. For the assessment of equivalent dose, 15 quartz aliquots of 1 mm were analysed from each sample.

The equivalent dose (D_e) data were evaluated by means of a radial plot (Galbraith 1990) together with sample-specific estimates of overdispersion (Galbraith et al. 2005). Considering the overdispersion values, D_e data were analysed using both the minimum age model (MAM) and the central age model (CAM) (Galbraith et al. 1999). Then, all results were assessed together with geological, geomorphologic, and sedimentological information from the study area. Environmental radioactivity dose values were assessed using the mass spectrometry at the laboratory of Mineral Research and Exploration General Directorate (MTA), and the annual dose values were calculated using U, Th, and K ratios the samples absorbed in a year.

Unfortunately, charcoal or organic material suitable for radiocarbon dating was not found in the sedimentary units that were studied.

4 Tuzla fault: definition and segment characteristics

The Tuzla Fault (TF), which is the main subject of the study, has been referred to with different names in the literature. Eşder and Şimşek (1975) used the name “Tuzla Fault” for the first time in their geothermal-based study. Kaya (1979 and 1981) states that NE-trending structural lineaments limit the Seferihisar and Çubukludağ sections. The same structural boundary named as Cumaovası lineaments (Şaroğlu et al. 1987, 1992), Cumalı reverse fault (Eşder 1988), Tuzla Fault (Emre and Barka 2000; Emre and Özalp 2011; Emre et al. 2011), and Orhanlı Fault Zone (Genç et al. 2001; Uzel and Sözbilir 2008).

In this work, we use the name “Tuzla Fault” (Eşder and Şimşek 1975; Emre and Barka 2000) as it was first described and defined on the Active Fault Map of Turkey. Emre and Barka (2000) define the fault as a NE–SW-trending structure between Gaziemir and Doğanbey in the south-west of İzmir. Uzel and Sözbilir (2008) described this fault as a main structural boundary within the IBTZ. The fault has a reported total length of 45 km (Uzel and Sözbilir (2008), whereas Emre et al. 2005; Ocakoğlu et al. 2004, 2005; Gürçay (2014) report that the TF continues on the floor of the Aegean Sea to the SW and its length exceeds 50 km. Uzel and Sözbilir (2008) present field data showing that the fault operated with left-lateral strike–slip in the Miocene and right-lateral strike–slip during the

Quaternary. Emre et al. (2005) state that the TF consists of three sub-sections. Researchers define these subdivisions as Çatalca (15 km), Orhanlı (16 km), and Cumalı (13 km) from north to south. According to the researchers, it is reported that the Cumalı (Doğanbey) section located in the south-west of the fault offers 10 km continuity on the Aegean Seafloor.

The fault plane at the Tuzla trench site cuts Quaternary travertines. The strike and dip of the fault were measured as N32E/77NW with a pitch of the slip line of 28° in the lower part, while the strike and dip of the fault were N40E/84NW and the pitch of the slip line was measured as 17° in the upper part (Fig. 3). Field observations and fault slip measurements in this site indicate that NE-SW-trending TF is a right-lateral strike–slip fault with a minor normal component during the Quaternary.

Measurements on fault planes observed during field studies document both the left- and right-lateral strike–slip character of the fault, as evidenced in previous studies (Uzel and Sözbilir 2008).

4.1 Rock units exposed along the Tuzla fault

The outcrops along the TF consist of three main rock assemblages separated from each other tectono-stratigraphically and stratigraphically. These are (1) pre-Miocene basement rocks, (2) Miocene basement rocks, and (3) Plio-Quaternary sedimentary rocks.

The Pre-Miocene basement rock units consists of 2 main rock assemblages, namely the Cycladic Complex generally composed of metasedimentary units which contain

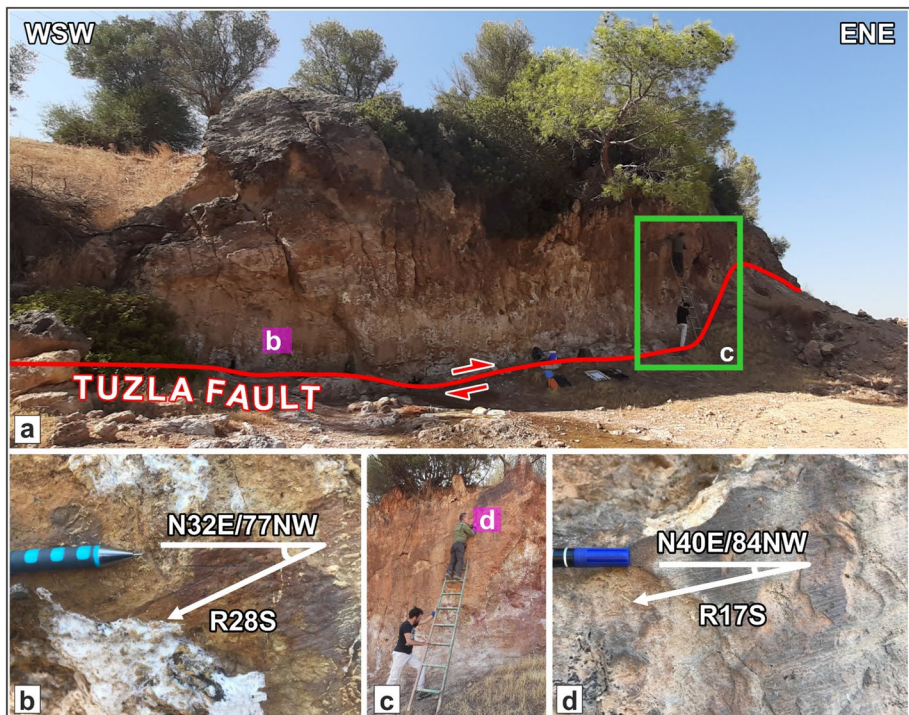


Fig. 3 Field view of Tuzla Fault (a) and (c), close-up view of slickenside fault surface (b) and (d)

metaserpentinite and metadiabase blocks and, the rock of İzmir—Ankara Zone made up of mudstone, sandstone, limestone, and conglomerate alternation in its matrix and containing limestone, basalt, diabase, and serpentinite blocks. Çetinkaplan et al. (2020), suggest that the epidote-blueschist metamorphism for the Cycladic Complex ranges between 57 and 40 Ma, and the overlying retrograde greenschist metamorphism between 35 and 32 Ma. The geological age of the rocks of the İzmir—Ankara Zone has been studied extensively in the literature (cf. Akartuna 1962; Özer and İrtəm 1982; Erdoğan 1990; Sarı, 2013; Okay et al. 2012). When all these studies are evaluated, it is seen that the depositional age of the unit is Upper Cretaceous–Palaeocene, and the blocks are distributed in the Triassic—Cretaceous age range.

The pre-Miocene basement rocks are unconformably overlain by Miocene aged sedimentary and volcanic units. The formations exposed along the south-eastern block of the TF as roughly Miocene age sedimentary units are composed of clastic to carbonate rock assemblages varying from conglomerate to limestone lithology. The products of Miocene volcanism are characterized by lava, dome, and pyroclastic facies varying from andesitic to rhyolitic in composition. Detailed description of these Miocene rocks is beyond the scope of this paper, and readers are referred to Göktaş (2019), Karacık and Genç (2013) for further details. The TF also creates an important structural boundary and juxtaposing together of Miocene aged sedimentary and volcanic units, and pre-Miocene sedimentary and metamorphic rock assemblages (Fig. 4).

All these older geological units are overlain by Plio-Quaternary sedimentary rocks. These semi-consolidated to unconsolidated units are made up of coarse-grained clastics and predominantly represented by alluvial and fluvial sedimentary facies, which are located in the south-eastern block of the TF, exposed from south-west to north-east in localities of the Buca, Gazimiri, Görece, and Ürkmez settlements, and these exposures have parallel characteristics with the main fault trend (Fig. 4).

5 Palaeoseismology

In order to reveal the earthquake history of the TF, we conducted three trench investigations from north to south at the Çatalca, Yeniköy, and Tuzla locations along the TF, respectively.

5.1 Çatalca trench

The Çatalca trench was excavated on the Çatalca segment of TF. To find an optimum trench location, we evaluated the neck cutoff along the fault that passes through the valley. The trench was opened roughly perpendicular to fault strike, with north-east and south-east trench walls of 24 and 23 m in length, respectively, and up to 3 m deep and wide (Figs. 4 and 5). Both trench walls exposed eleven units with recent soil cover. The subdivided first three units were evaluated as basement units, namely A, B1, and B2. Unit A is the rock unit belonging to the Upper Cretaceous–Palaeocene aged İzmir—Ankara Zone shown on the geological map (Fig. 4). Unit A consists of whitish-dark grey mud shale, claret-light brown–grey mudstone, and milky pinkish brown poorly sorted sandstone. Unit A is laterally traced between 0 and 20 m horizontal scale marks of the trench walls. Moreover, it is clearly seen that mudstone and mud shale interfinger between 5 and 7 m of the horizontal scale marks of the trench walls. The sandstones are mostly seen as lenses formed as a boudinage structure in the shear zone. This unit has been folded and cut by multiple

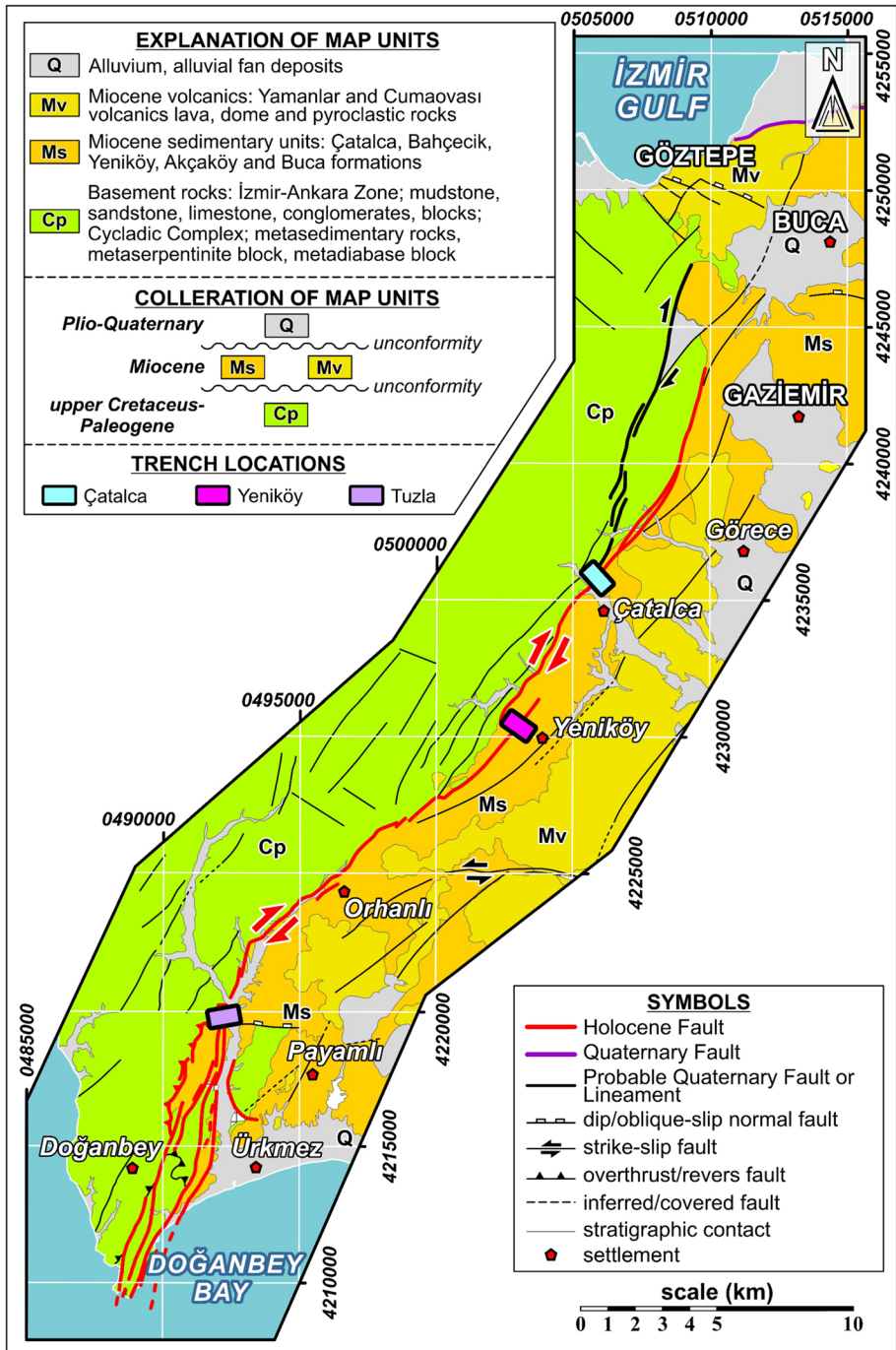


Fig. 4 Geological map of Tuzla Fault (prepared from Göktaş and Çakmaköğlu 2018; Göktaş, 2019 and data from this study)

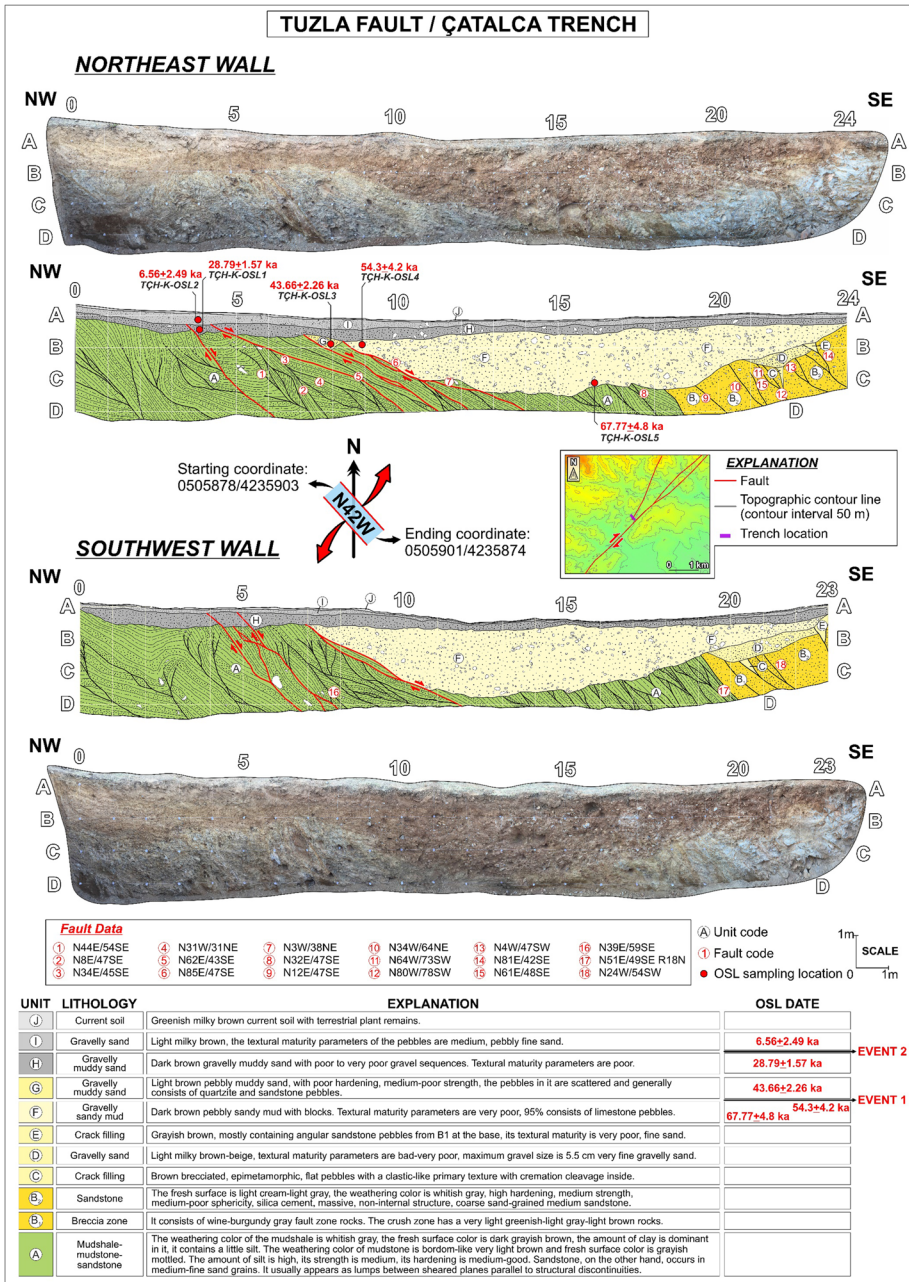


Fig. 5 Photomosaic and palaeoseismology log of the Çatalca trench

fault zones, which is defined for the TF between 19 and 20 m horizontal scale marks of the trench walls. Unit B1 and unit B2 are the Miocene aged sedimentary rocks shown on the geological map (Fig. 4). Unit B1 represents light green-light brown and claret grey,

unsorted breccia derived from sandstone between 19 and 20 m horizontal scale marks of the trench walls. Similarly, unit B2 consists of light brown–grey, unsorted sandstone with coarse sand. These units are overlain by brown, unsorted, brecciated gravel derived from epimetamorphic rocks (Unit C) between 21 and 22 m horizontal marks of the trench walls, light brown-beige, poorly matured fine grain sand (Unit D) ranging from 19 to 23 m of the horizontal marks of the trench walls, and greyish brown, poorly matured gravel derived from B1 (Unit E). Furthermore, unit C and unit E represent crack fills. Units A through E are unconformably overlain by dark brown, poorly matured, unsorted gravelly muddy sand (Unit F) between 6 and 24 m of the trench walls. The gravels are derived from limestone lithology. The overlying unit G represents light brown, unsorted gravelly muddy sand. This unit is located on the hanging wall of the NE-directed fault as a colluvial wedge between 7 and 8 m within the north-east wall. Similarly, the previous units are unconformably overlain by unit H. It consists of dark brown unsorted gravelly muddy sand and is cut by SE dipping faults. The overlying unit I consists of light milky brown unsorted fine grained gravelly sand. Finally, all these units are unconformably overlain by light to dark brown recent soil with organic-rich material (Unit J). The faults observed in both trench walls are compatible with each other. In addition, the black lines shown in the trench log in Fig. 5 indicate cleavage fractures in the unit.

A total of five OSL samples were collected from the Çatalca trench within the north-east wall. The derived dates of the samples from the trench exposures were dated between 6.56 ± 2.49 ka and 67.77 ± 4.80 ka (Table 2). Based on the sedimentological and stratigraphic evidence for the analysis of structural elements together with the results of dated samples, two events were identified in the Çatalca trench. The earliest event occurred after the deposition of unit F and before the deposition of unit G. Hence, we collected an OSL sample from unit G (sample number TÇH-K3) representing the upper boundary of the first event, which yielded a date of 43.66 ± 2.26 ka, and from unit F (sample number TÇH-K4) representing the lower boundary of the first event, which yielded a date of 54.3 ± 4.2 ka. The final event cuts unit H, so it occurred after the deposition of unit H and before the deposition of unit I. Thus, the sample collected from unit H (TÇH-K1) yielded an OSL date of 28.79 ± 1.57 ka, representing the lower boundary of the second event, while the sample collected from the overlying unit I (TÇH-K2) yielded a date of 6.56 ± 2.49 ka (Fig. 5).

5.2 Yeniköy trench

The Yeniköy trench was excavated perpendicular to the fault strike (Fig. 4). It was 24 m long, 3.5 m wide and deep, opened on the Orhanlı segment of TF, and revealing eight stratigraphic units (Fig. 6). The basement unit (A), consists of the interfingering of reddish brown, unsorted, matrix-supported sandy conglomerate, with tuffites, sandstone, and pyroclastic gravels, wine-brown fine gravelly coarse sandy mudstone, and lastly milky brown unsorted fine gravel derived from sandstone, mudstone, and chert. The Miocene unit A is laterally traced between 0 and 24 m of the trench walls. This unit was cut by a fracture calcite fill between 22 and 23 m of the north-east wall. Further, while a uniform trend of Unit A was observed in the middle section of the trench walls, it was otherwise deformed by a set of faults. Unit A is overlain by Unit B with an angular unconformity. Unit B consists of dark brown poorly matured, unsorted sandy matrix-supported coarse gravel. The overlying unit C comprises light brown sandstone with fine gravels derived from sandstone. These units are overlain by brown, unsorted, poorly matured matrix-supported coarse gravel derived from the sandstone, limestone, and mudstone (Unit D) between 4 and 24 m of the

Table 2 Sample information, equivalent dose (D_e), dose rate data, and quartz OSL ages calculated for samples collected from the three trenches on the Tuzla Fault

Study area	Sample No	Grain size (μm)	Radioelement data		Water Content (%)	Altitude (m)	Depth (cm)	Coordinate (Decimal Degrees) ($^{\circ}\text{N}$, $^{\circ}\text{E}$)	Equivalent Dose (D_e (Gy))	Dose-Rate (Gy/ka)	Age (ka)
			U (ppm)	Th (ppm)							
Izmir Tuzla Trench	TT-1	125–180	0.4	3.7	1.04	58	263	$38.1013^{\circ}-26.9023^{\circ}$	6.70 ± 0.76	1.22 ± 0.05	5.51 ± 0.67
	TT-2	125–180	0.5	1.6	1.16	58	375	$38.1013^{\circ}-26.9023^{\circ}$	1.31 ± 0.68	1.47 ± 0.08	0.89 ± 0.46
	TT-3	125–180	0.3	2.9	0.99	58	193	$38.1013^{\circ}-26.9023^{\circ}$	8.80 ± 1.00	1.16 ± 0.05	7.61 ± 0.92
	TT-6	125–180	0.3	2	2.20	58	275	$38.1013^{\circ}-26.9023^{\circ}$	5.00 ± 3.50	1.96 ± 0.08	2.55 ± 1.78
	TT-9	125–180	0.4	3	0.95	58	230	$38.1013^{\circ}-26.9023^{\circ}$	8.48 ± 0.45	1.18 ± 0.05	7.19 ± 0.49
	Çatalca Trench	TÇH-1	125–180	0.6	5.9	1.04	195	25	$38.2654^{\circ}-27.0643^{\circ}$	40.70 ± 1.50	1.41 ± 0.05
TÇH-2		125–180	0.4	4.1	1.16	195	58	$38.2654^{\circ}-27.0643^{\circ}$	8.50 ± 3.20	1.30 ± 0.05	6.56 ± 2.49
TÇH-3		125–180	0.4	5.5	0.99	195	65	$38.2654^{\circ}-27.0643^{\circ}$	59.30 ± 2.00	1.36 ± 0.05	43.66 ± 2.26
TÇH-4		125–180	0.3	1.7	0.99	195	72	$38.2654^{\circ}-27.0643^{\circ}$	55.60 ± 3.50	1.02 ± 0.04	54.30 ± 4.20
Yeniköy Trench	TÇH-5	125–180	0.3	2.5	1.16	195	200	$38.2654^{\circ}-27.0643^{\circ}$	89.00 ± 2.40	1.31 ± 0.05	67.77 ± 4.80
	TYH-1	150–250	0.1	2.6	1.25	193	185	$38.2241^{\circ}-27.0394^{\circ}$	23.90 ± 2.10	1.40 ± 0.06	17.05 ± 1.69
	TYH-2	150–250	0.2	3	1.17	193	250	$38.2241^{\circ}-27.0394^{\circ}$	15.60 ± 2.70	1.25 ± 0.06	12.51 ± 2.24
	TYH-3	150–250	0.1	2.2	1.06	193	163	$38.2241^{\circ}-27.0394^{\circ}$	27.20 ± 1.90	1.08 ± 0.04	25.20 ± 2.04
	TYH-4	150–250	0.1	2.3	0.94	193	138	$38.2241^{\circ}-27.0394^{\circ}$	182.00 ± 13.00	1.03 ± 0.05	176.32 ± 15.14
	TYH-5	150–250	0.5	1	0.58	193	235	$38.2241^{\circ}-27.0394^{\circ}$	27.30 ± 2.40	0.74 ± 0.04	37.04 ± 3.74
	TYH-6	150–250	0.2	1.8	0.85	193	250	$38.2241^{\circ}-27.0394^{\circ}$	20.50 ± 1.50	0.86 ± 0.04	23.92 ± 2.09
TYH-7	150–250	0.1	1.3	0.75	193	248	$38.2241^{\circ}-27.0394^{\circ}$	1.53 ± 0.63	0.87 ± 0.04	1.77 ± 0.77	

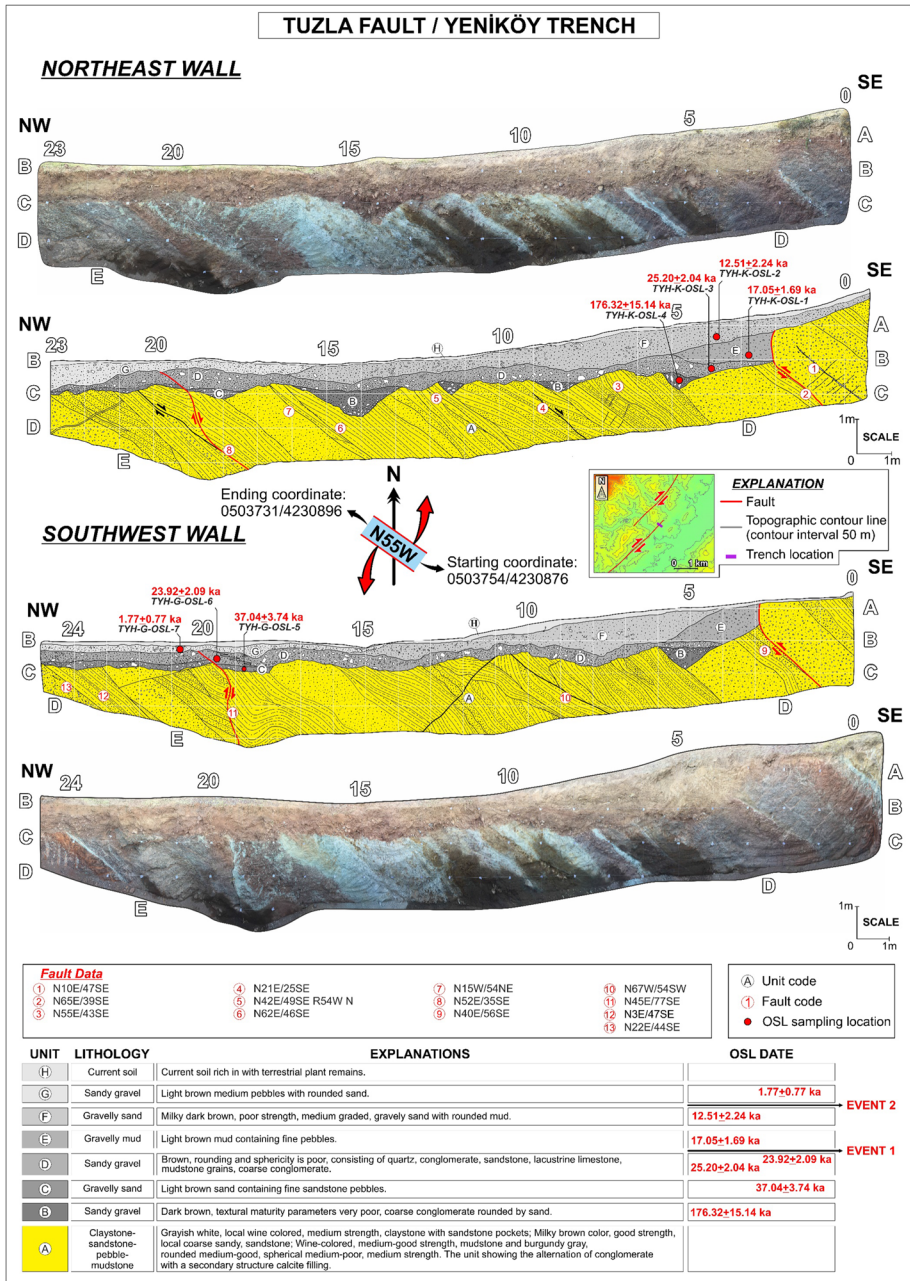


Fig. 6 Photomosaic and palaeoseismology log of the Yeniköy trench

trench walls; light brown fine gravelly mud (Unit E) ranged from 3 to 6 m in trench walls. Unit D is cut by a SE dipping fault. The previous units are overlain by milky-dark brown, moderately matured gravelly sand (Unit F). While unit F is observed in the first 15 m

within the north-east wall, it is only clearly visible between 4 and 15 m of the south-west wall. The overlying unit G consists of a light brown moderately matured sandy matrix-supported conglomerate. Lastly, all these units are unconformably overlain by dark brown soil with organic-rich material and there is no evidence that this unit was cut by faults (unit H).

We collected seven OSL samples from the Yeniköy trench exposures. The derived dates of the samples from the trench were dated between 176.32 ± 15.14 ka and 1.77 ± 0.77 ka (Table 2). Based on the results of the dated samples together with the sedimentological and stratigraphic evidence for the analysis of the structural elements, it was seen that the faults identified in the Yeniköy trench may belong to the same or two different earthquakes. The relationship between Event 2 and unit F shown in Fig. 6 can be interpreted as follows: (1) Unit F was deposited after event 2 occurred; (2) Event 2 occurred after unit F was deposited. Within the scope of this study, Yeniköy trench was interpreted according to the earthquake scenario numbered 2. The penultimate event occurred after the deposition of unit D and before the deposition of unit E. So, to define the lower boundary of the event, we collected sample TYH-6 from unit D, yielding a date of 23.92 ± 2.09 ka. The OSL age from the base of unit E (TYH-1; 17.05 ± 1.69 ka) gives the upper boundary of the event in the Yeniköy trench. The final event occurred after the deposition of unit F and before the deposition of unit G. Thus, the samples collected from unit F (TYH-2) yielded an OSL date of 12.51 ± 2.24 ka representing the lower boundary of the second event while the samples collected from the overlying unit G (TYH-7) yielded a date of 1.77 ± 0.77 ka (Fig. 6).

5.3 Tuzla trench

The Tuzla trench was excavated on the Doğanbey segment of TF (Fig. 4). A trench was placed across the fault strike, and the north-east trench wall was nearly 10 m long, up to 4 m deep, 3 m wide, and we logged 8-m of the 10-m-long trench walls. Because there is no change in units, the last 2 m were not logged (Fig. 7). Geothermal fluids were present in the bottom of the trench exposures; thus, we could not excavate more deeply. The basement unit (Unit A) consists of reddish brown fine sandstone and reddish dark brown mudstone alternating with brownish-green mudstone. Further, it is deformed by several faults and there is observable manganese dendrite on this unit. It was unconformably overlain by unit B. Unit B consists of a brownish reddish organic-rich palaeosol cut by a fault. The measured vertical displacement is up to 10 cm between 3 and 4 m of the trench walls. The overlying unit C represents pinkish light brown unsorted and poorly matured sandy gravel. It has an openwork structure on the south-east wall. These units are overlain by reddish brown poorly matured and poorly strengthened fine gravelly sand (Unit D) that is clearly observable between 2 and 4 m of the trench wall as a crack fill; a reddish brown palaeosol (Unit E) is observable in the first 5 m of south-east wall. The overlying unit F is characterized by yellowish-light brown unsorted, poorly matured, and muddy matrix-supported blocky coarse gravel derived from sandstone with manganese, silicified sandstone, and fault rocks. It has an openwork structure—a colluvial wedge—and is clearly observable in the first 1 m of the south-east wall. Similarly, the overlying unit G represents pinkish light brown sandy unsorted and poorly matured sandy gravel. Units E through G are not observed in the north-west trench wall due to possible erosional processes. Lastly, all these units are unconformably overlain by light yellowish brown soil with fine gravel (unit H).

We identified three events in the Tuzla trench, based on the sedimentological and stratigraphic evidence for the analysis of structural elements together with the results of dated samples. The derived dates of the samples from the Tuzla trench were dated between

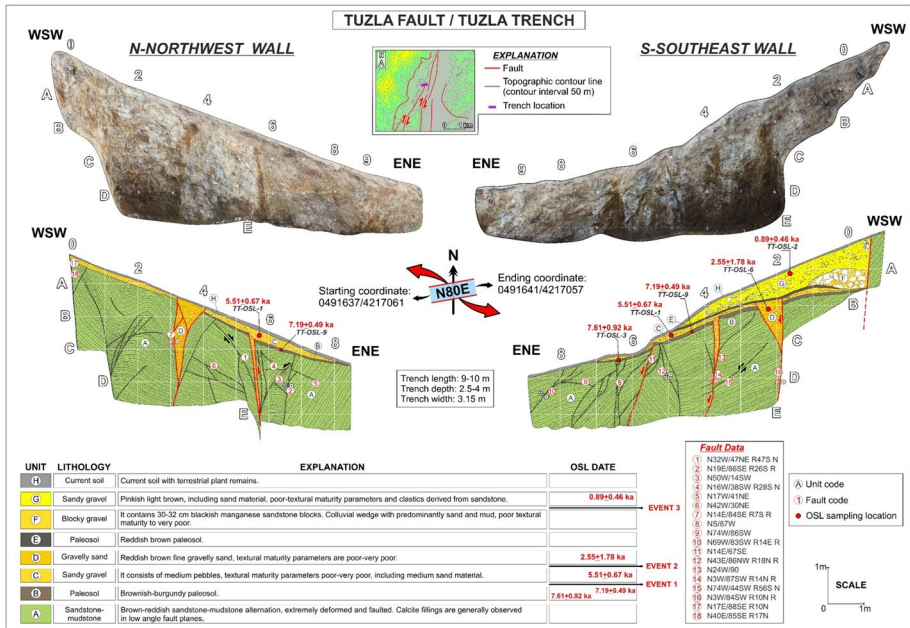


Fig. 7 Photomosaic and palaeoseismology log of the Tuzla trench

0.89 ± 0.46 ka and 7.61 ± 0.92 ka (Table 2). The earliest event after the deposition of unit B and before the deposition of unit C. We collected an OSL sample from unit C (TT-1) representing the upper boundary of the first event, which yielded a date of 5.51 ± 0.67 ka, and from unit B (TT-9) representing the lower boundary of the first event, which yielded a date of 7.19 ± 0.49 ka. The penultimate event occurred after the deposition of unit C and before the deposition of unit D. Thus, the sample collected from unit C with OSL date of 5.51 ± 0.67 ka (TT-1) represents the lower boundary of the second event, while the sample collected from the overlying unit D (TT-6) yielded a date of 2.55 ± 1.78 ka. The final event occurred after the deposition of unit E and before the deposition unit F. Unfortunately, we could not find sufficient material to date the lower unit E and upper unit F. Our ages for units D and G help constrain the event, to an age between 2.55 ± 1.78 ka and 0.89 ± 0.46 ka for units D and G, respectively (Fig. 7).

5.4 Palaeoseismology interpretations

Based on the well-constrained earthquake events within the three trenches we assume that seven earthquake cycles have occurred on the TF. According to Oxcal distribution using Bayesian methods, the events are E1: 46.2 ± 6.1 ka; E2: 30.4 ± 7.2 ka; E3: 16.3 ± 4.1 ka; E4: 9.1 ± 2.3 ka; E5: 4.9 ± 0.7 ka; E6: 2.7 ± 0.7 ka; and E7: 1.6 ± 0.3 ka (Fig. 8). When the events are compared with the historical earthquakes, the E7 event may correlate with the earthquakes of 47 AD and/or 177/178 AD. Moreover, the E1–E6 events can be attributed to the prehistoric BC earthquakes that originated on the fault but are not included in the historical catalogues (Table 3). More so, in the light of the historic/prehistoric earthquakes generated by the TF, the recurrence interval was found to be between 0.7 and 4.3 ka for the

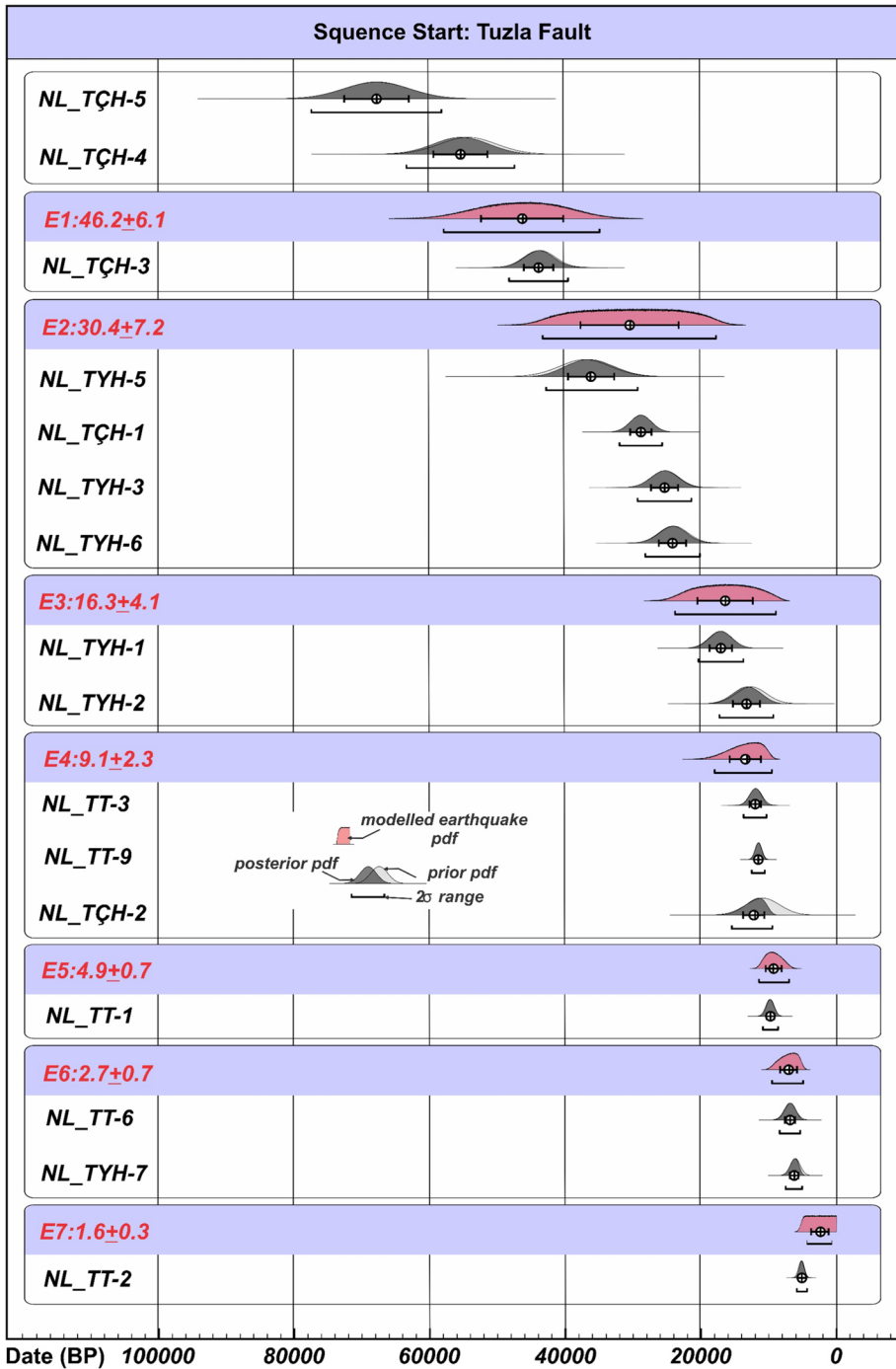


Fig. 8 Preferred model from OxCal v4.4.4 (Ramsey 2008, 2009; Reimer et al. 2009) of timing constraints on earthquakes (E1–E7) at T1–T3 trenches on the Tuzla Fault. Ages listed in sequence are in stratigraphic order, without depth constraints. Prior probability distribution function (Pdf) ages are defined by the calibrated OSL ages. Posterior Pdf ages are calculated from the Bayesian OxCal analysis

Table 3 Event timing in the Çatalca, the Tuzla, and the Yeniköy trenches along the Tuzla Fault and corresponding earthquakes

	Event	%95.4–2 sigma-modelled with Oxcal	Historical Earthquake
Çatalca Trench	E1	47,380 BC-31800 BC	–
	E2	18,280 BC-5680 BC	–
Tuzla Trench	E1	4380 BC-2000 BC	–
	E2	2000 BC-420 AD	47 AD
	E3	120 AD-1320 AD	177/178 AD
Yeniköy Trench	E1	18,280 BC-6680 BC	–
	E2	4780 BC-600 BC	–

Holocene, and the elapsed time since the most recent surface ruptured earthquake on the TF is 1845 years (Table 4).

6 Discussion and conclusion

The NE striking Tuzla Fault (TF) is one of the most important seismic sources in İzmir province. The TF has a strike–slip mechanism within the Western Anatolian Graben System and is made up of three active segments between Gaziemir and Doğanbey districts. In order to reveal (i) earthquake history of the TF, (ii) the earthquake recurrence interval models, and (iii) elapsed time since the most recently occurred surface rupture, three

Table 4 Earthquake timing, interevent time, and recurrence interval in the eastern segment of the Tuzla Fault

E ^a	Event Times			Time Between Events			Recurrence Interval ^b								
	A (ka)			I (ka)(AE _{first} -AE _{second})			R (ka)								
	A _{min}	A _{average}	A _{max}	I _{min}	I _{average}	I _{max}	R _{Holocene}			R _{Pleistocene}			R _{Holisticly}		
			(AE _{min} -AE _{max})	(AE _{average} -AE _{average})	(AE _{max} -AE _{min})	R _{min}	R _{average}	R _{max}	R _{min}	R _{average}	R _{max}	R _{min}	R _{average}	R _{max}	
E1	40.1 ^P	46.2 ^P	48.3 ^P	2.5 ^{PE}	15.8 ^{PE}	25.1 ^{PE}	0.7	2.5	4.3	2.0	12.4	21.4	1.4	7.4	12.8
E2	23.2 ^P	30.4 ^P	37.6 ^P	2.8 ^{PE}	14.1 ^{PE}	25.4 ^{PE}									
E3	12.2 ^P	16.3 ^P	20.4 ^P	0.8 ^{PE}	7.2 ^{PE}	13.6 ^{PE}									
E4	6.8 ^H	9.1 ^H	11.4 ^H	1.2 ^{HE}	4.2 ^{HE}	7.2 ^{HE}									
E5	4.2 ^H	4.9 ^H	5.6 ^H	0.8 ^{HE}	2.2 ^{HE}	3.6 ^{HE}									
E6	2.0 ^H	2.7 ^H	3.4 ^H	0.1 ^{HE}	1.1 ^{HE}	2.1 ^{HE}									
E7	1.3 ^H	1.6 ^H	1.9 ^H												

a: According to preferred model derived from Oxcal (Ramsey 2008, 2009; Reimer et al. 2009).

b*: Represents recurrences interval based on the formula (Duran et al. 2021).

The formula:

$$R_{min}: (AE1_{min}-AE2_{max}) + (AE2_{min}-AE3_{max}) + (AE3_{min}-AE4_{max})/n-1$$

$$R_{average}: (AE1_{average}-AE2_{average}) + (AE2_{average}-AE3_{average}) + (AE3_{average}-AE4_{average})/n-1$$

$$R_{max}: (AE1_{max}-AE2_{min}) + (AE2_{max}-AE3_{min}) + (AE3_{max}-AE4_{min})/n-1$$

E Events, N number of events, H Holocene, P Pleistocene, HE Holocene Event, PE Pleistocene Event

trench-based palaeoseismology studies were performed on the TF. Based on this current research, the following assessments and discussions can be made.

The palaeoseismology studies in the Çatalca trench, which is on the Çatalca segment of TF, indicate that this segment is responsible for two events between 6.56 ± 2.49 ka and 54.3 ± 4.2 ka. Neither the penultimate nor the final event identified from this trench can be attributed to a historical earthquake. It may fit prehistoric/or undefined earthquakes.

Palaeoseismology data from the Yeniköy trench on the central segment of TF, provides evidence for two events after 23.92 ± 2.09 ka. Similarly, while two events were observed in Yeniköy trench, a historical earthquake record was not observed. Although these events are too old to correlate with historical earthquake catalogues, our results show clear evidence that the TF is responsible for two large earthquakes in prehistory in the relevant segment.

Palaeoseismology evidence from the Tuzla trench on the Tuzla segment of TF reveals three events were observed between 0.89 ± 0.46 ka and 7.61 ± 0.92 ka. For the first event observed in Tuzla trench, there is no record of any large earthquake in Izmir region between 5.51 ± 0.67 ka and 7.19 ± 0.49 ka. The penultimate event took place sometime between 2.55 ± 1.78 ka and 5.51 ± 0.67 ka, which can be correlated with the 47 AD earthquake considering the historical earthquake catalogues. The last event can be the best fit for the 177/178AD earthquake.

TF comprises three geometric segments, namely Çatalca, Orhanlı, and Tuzla. Due to the fact that the fault reflects differing behaviour at these three segments, we performed separate palaeoseismological studies at all three segments. We identified two, three, and two events on the Çatalca, Tuzla, and Orhanlı segment, respectively. We assumed that seven earthquake cycles have occurred on the TF in the Holocene and Pleistocene time interval. These events are E1: 46.2 ± 6.1 ka; E2: 30.4 ± 7.2 ka; E3: 16.3 ± 4.1 ka; E4: 9.1 ± 2.3 ka; E5: 4.9 ± 0.7 ka; E6: 2.7 ± 0.7 ka; and E7: 1.6 ± 0.3 ka. Considering these fault events, we refined our data using the Oxcal program with the Bayesian methods. From this point on, we inferred seven events, when evaluated together with three segments, with recurrence interval between 0.7 and 4.3 ka for the Holocene, and the elapsed time since the most recent surface ruptured earthquake on the TF is 1845 years.

The error limits of the dating methods (OSL, TL) are usually ± 5 to $\pm 10\%$ of the age (Aitken 1997). OSL dating is possible over a wide age range of a few decades to about half a million years, although uncertainties are usually relatively larger towards the extremes of this age range. Mainly due to systematic errors in both dose rate (conversion factors) and equivalent dose (source calibration) estimation. In most cases, the uncertainty will be higher due to random errors (e.g. spread in equivalent doses) or uncertainty in assumptions (e.g. water content fluctuations, burial history) (Wallinga and Cunningham 2014). Some luminescence dating studies have shown that the age -related errors may even be around 25%. Wide margins of error in such cases are known to arise due to the uncertainty associated with the gamma dose rate used in calculating the annual dose (Duller 2003).

For this reason, it is thought that high error rates are expected for samples with close (young sediments) or very distant (old sediments) time since daylight resetting, and the geological interpretation of the event with these age data is considered to be more important.

In this study, the recurrence interval was delineated by the obtained robust OSL age data. Besides the OSL age data, the recurrence interval depends on sedimentary sequences in dynamic environments where the sedimentation rate is highly variable (e.g. Berryman et al. 2012; Kempf and Moernaut 2021). The general problem of the uncertainty regarding the lower and upper bounds of recurrence interval in western Anatolia may generated from the variable sedimentation rate as such 1.1 mm/year (e.g. Westaway 1994).

Table 5 According to Wells and Coppersmith (1994) equations, maximum earthquake generation potentials of Tuzla Fault segments. Note that the *a* and *b* variables are the constant coefficients

Magnitude (M) = $a + [b \cdot \log(\text{fault length})]$					
Fault segment	<i>a</i>	<i>b</i>	Fault length (km)	Log (fault length)	Magnitude (M _w)
Çatalca segment	5.16	1.12	15.75	1.1973	6.50
Orhanlı segment			16.25	1.2109	6.52
Doğanbey segment			12.35	1.0917	6.38
All segments			55	1.7404	7.11

According to the previously published studies, earthquake hazard mitigation is revealed from the palaeoseismological (e.g. Şengöçmen Geçkin et al. 2022), seismological (e.g. Bayrak and Bayrak 2012; Akkar et al. 2018; Nas et al. 2020), and geodetic studies (e.g. Çirmik et al. 2017; Eyübagil et al. 2021; Aktuğ et al. 2021) along the strike–slip faults (Gülbağçe Fault-GF, Tuzla Fault-TF, Yağcılar Fault-YF) within İBTZ. From these faults, GF was studied by Şengöçmen Geçkin et al. (2022). They stated that GF is responsible for four surface rupturing earthquakes since the Late Pleistocene–Holocene and the last earthquake on this fault occurred 1389 AD with respect to historical catalogues. Further, the recurrence interval was found between 1.4 ka and 6.2 ka for the Holocene.

Similarly, Eyübagil et al. (2021) stated that in the region of the TF, while the geodetic earthquake recurrence period moment magnitude ranging from 6 to 6.5 was approximately 150–200 years, but this period for $M_w > 6.5$ and $M_w > 7$ was approximately 795 years and 3160 years, respectively. Moreover, GPS velocities were found under 1 mm/y around the TF. When evaluating these recurrence interval data obtained from their geodetic and our palaeoseismology studies signifies both results for mitigation techniques are in concordance with each other along the TF.

It is noted that TF has earthquake potential up to magnitude of 7.11, according to the Wells and Coppersmith (1994) equations as listed in Table 5. Considering the average recurrence interval suggest that TF can be grouped as class B, according to taxonomy of Slemmons and Depolo (1986). This diagram reveals that TF have moderate activity rate with moderate to well-developed geomorphic evidence of activity. Further, it indicates that the annual long term of slip rate is between 0.1 and 1 mm/y.

As powerfully articulated by Aktuğ et al. (2021) and Şengöçmen Geçkin et al. (2022), after the Samos earthquake ($M_w:6.9$), the seismicity flocculated on the TF and nearest region between 2020 and 2023 because of the stress transferred to the hanging wall of the Samos Fault. Further, hot water outflows during the post-earthquake along the SE edge of TF (Uzelli et al. 2021) and recently having occurred the seismicity along NE edge of TF, emphasized that TF has a more complex structure than observed and thought. Furthermore, after the 30 October 2020 ($M_w:6.9$) earthquake, the stress may be transferred to the hanging wall of the Samos fault where the TF, Gülbağçe Fault Zone, Seferihisar Fault, and Yağcılar Fault are located. This circumstance draws attention to the importance of the strike–slip fault mechanism in Western Anatolia Graben System. Ultimately, as is strongly stated by Şengöçmen Geçkin et al. (2022), it is highly recommended that palaeoseismological studies should be performed on these fault segments.

Acknowledgements This study is part of a master's thesis undertaken by the first author, is supervised by the second author at the Institute of Natural and Applied Sciences, Dokuz Eylül University, Turkey. This

research was supported by TÜBİTAK (The Scientific and Technological Research Council of Turkey) with project Number 117Y190, and by the Research Fund (BAP) of Çukurova University, Turkey, Project Number: FAY-2022-14782. The authors are grateful to BAP of Çukurova University. Thanks to anonymous referees for criticisms made during the evaluation phase of the manuscript. Their suggestions improved the article considerably. We would also like to thank the editor Francesco Comiti for his success in managing the article evaluation process.

Funding Open access funding provided by the Scientific and Technological Research Council of Türkiye (TÜBİTAK).

Declarations

Conflict of interest The authors have no relevant financial or non-financial interests to disclose.

Open Access This article is licensed under a Creative Commons Attribution 4.0 International License, which permits use, sharing, adaptation, distribution and reproduction in any medium or format, as long as you give appropriate credit to the original author(s) and the source, provide a link to the Creative Commons licence, and indicate if changes were made. The images or other third party material in this article are included in the article's Creative Commons licence, unless indicated otherwise in a credit line to the material. If material is not included in the article's Creative Commons licence and your intended use is not permitted by statutory regulation or exceeds the permitted use, you will need to obtain permission directly from the copyright holder. To view a copy of this licence, visit <http://creativecommons.org/licenses/by/4.0/>.

References

- Aitken MJ (1997) Luminescence dating. Chronometric dating in archaeology. Springer, US, Boston, MA, pp 183–216
- Aitken MJ (1998) Introduction to optical dating: the dating of Quaternary sediments by the use of photon-stimulated luminescence. Clarendon Press
- Akartuna M (1962) İzmir-Torbalt-Seferihisar-Urla Bölgesinin Jeolojisi Hakkında. Maden Tetkik Ve Arama Dergisi 59:1–18
- Akçar N, Tikhomirov D, Özkaymak Ç, Ivy-Ochs S, Alfimov V et al (2012) Cl-36 exposure dating of paleoearthquakes in the Eastern Mediterranean: first results from the western Anatolian Extensional Province, Manisa fault zone, Turkey. GSA Bull 124(11–12):1724–1735. <https://doi.org/10.1130/B30614.1>
- Akkar S, Azak T, Çan T, Çeken U, Demircioğlu Tümsa MB et al (2018) Evolution of seismic hazard maps in Turkey. Bull Earthq Eng 16:3197–3228
- Aktuğ B, Nocquet JM, Cingöz A, Parsons B, Erkan Y et al (2009) Deformation of western Turkey from a combination of permanent and campaign GPS data: limits to block-like behavior. J Geophys Res Solid Earth. <https://doi.org/10.1029/2008JB006000>
- Aktuğ B, Parmaksız E, Kurt M, Lenk O, Kılıçoğlu A, Gürdal MA, Özdemir S (2013) Deformation of central anatolia: GPS implications. J Geodyn 67:78–96
- Aktuğ B, Tiryakiyoğlu İ, Sözbilir H, Özener H, Özkaymak Ç et al (2021) GPS derived finite source mechanism of the 30 October 2020 Samos earthquake, Mw =6.9, in the Aegean extensional region. Turk J Earth Sci. <https://doi.org/10.3906/yer-2101-18>
- Akyüz HS, Kırcan E, Basmenji M, Aksoy E, Akyüz AD et al. (2019) Paleoseismological and morphotectonic characteristics of active faults in the vicinity of Muğla Area (SW Turkey). In: On significant applications of geophysical methods: proceedings of the 1st Springer Conference of the Arabian Journal of Geosciences (CAJG-1), Tunisia 2018, Springer International Publishing, pp 253–256
- Akyüz HS, Uçarkuş G, Şatır D, Dikbaş A, Kozacı Ö (2006) 3 Şubat 2002 Çay depreminde meydana gelen yüzey kırığı üzerinde paleoseismolojik araştırmalar. Yerbilimleri Dergisi 27(1):41–52 ((in Turkish))
- Altunel E, Barka A, Akyüz S (1999) Palaeoseismicity of the Dinar fault. SW Turkey Terra Nova 11(6):297–302. <https://doi.org/10.1046/j.1365-3121.1999.00262.x>
- Ambraseys NN (2009) Earthquakes in the Mediterranean and Middle East: a multidisciplinary study of seismicity up to 1900. Cambridge University Press, Cambridge, United Kingdom
- Ambraseys NN, Finkel C (1995) The seismicity of Turkey and adjacent areas: a historical review, 1500–1800. İstanbul, Eren

- Ambraseys NN, Jackson JA (1998) Faulting associated with historical and recent earthquakes in the Eastern Mediterranean region. *Geophys J Int* 133(2):390–406. <https://doi.org/10.1046/j.1365-246X.1998.00508.x>
- Armijo R, Meyer B, Hubert-Ferrari A, Barka A (1999) Westward propagation of North Anatolian Fault into the Northern Aegean: timing and kinematics. *Geology* 27:267–270
- Barka AA (1992) The North Anatolian fault zone. *Annales Tectonicae* 6:164–195
- Barka AA (1999) The 17 August 1999 İzmit earthquake. *Science* 285:1858–1859
- Basmenji M, Akyuz HS, Kirkan E, Aksoy ME, Ucarukus G et al (2021) Earthquake history of the Yatagan Fault (Muğla, SW Turkey): implications for regional seismic hazard assessment and palaeoseismology in extensional provinces. *Turk J Earth Sci* 30(2):161–181. <https://doi.org/10.3906/yer-2006-23>
- Başarır Baştürk N, Özel NM, Altınok Y, Duman TY (2016) Türkiye ve yakın çevresi için geliştirilmiş tarihsel dönem (MÖ 2000-MS 1900-) deprem katalogu. *Türkiye Sismotektonik Haritası Açıklama Kitabı*, MTA Özel Yayınlar Serisi-35, 287 s. Ankara, 2016 (in Turkish)
- Bayrak Y, Bayrak E (2012) An evaluation of earthquake hazard potential for different regions in Western Anatolia using the historical and instrumental earthquake data. *Pure Appl Geophys* 169:1859–1873
- Berryman KR, Cochran UA, Clark KJ, Biasi GP, Langridge RM et al (2012) Major earthquakes occur regularly on an isolated plate boundary fault. *Science* 336(6089):1690–1693
- Bookhagen B, Echtler HP, Melnick D, Strecker MR, Spencer JQG (2006) Using uplifted Holocene beach berms for paleoseismic analysis on the Santa María Island, south-central Chile. *Geophys Res Lett* 33:L15302. <https://doi.org/10.1029/2006GL026734>
- Bürgmann R, Segall P, Lisowski M, Svarc J (1997) Postseismic strain following the 1989 Loma Prieta earthquake from GPS and leveling measurements. *J Geophys Res: Solid Earth* 102(B3):4933–4955
- Campbell KW (1982) Bayesian analysis of extreme earthquake occurrences. Part I. Probabilistic hazard model. *Bull Seismol Soc Am* 72(5):1689–1705
- Caputo R, and Pavlides S (2013) The Greek database of seismogenic sources (GreDaSS), version 2.0. 0: a compilation of potential seismogenic sources (Mw > 5.5) in the Aegean Region. University of Ferrara: Ferrara, Italy
- Chen Y, Hu J, Peng F (2018) Seismological challenges in earthquake hazard reductions: reflections on the 2008 Wenchuan earthquake. *Sci Bull* 63(17):1159–1166
- Çetinkaplan M, Candan O, Oberhänsli R, Sudo M, Cenk-Tok B (2020) P-T-t evolution of the Cycladic Blueschist Unit in Western Anatolia/Turkey: geodynamic implications for the Aegean region. *J Metamorph Geol* 38(4):379–419
- Çırmık A, Pamukçu O, Gönenç T, Kahveci M, Şalk M et al (2017) Examination of the kinematic structures in İzmir (Western Anatolia) with repeated GPS observations (2009, 2010 and 2011). *J Afr Earth Sc* 126:1–12
- Dikbaş A, Akyüz HS, Basmenji M, Kirkan E (2022) Earthquake history of the Gökova fault zone by paleoseismologic trenching, SW Turkey. *Nat Hazards*. <https://doi.org/10.1007/s11069-022-05284-0>
- Doğan T, Cetin H, Yegingil Z, Topaksu M, Yüksel M et al (2015) Optically stimulated luminescence dating of Holocene alluvial fans, East Anatolian Fault System, Turkey. *Radiat Eff Defects Solids* 170(7–8):630–644. <https://doi.org/10.1080/10420150.2015.1077333>
- Duller GAT (2003) Distinguishing quartz and feldspar in single grain luminescence measurements. *Radiat Meas* 37(2):161–165
- Duman TY, Çan T, Emre Ö, Kadıroğlu F, Başarır Baştürk N et al (2018) Seismotectonic database of Turkey. *Bull Earthq Eng* 16(8):3277–3316
- Duman TY, Emre Ö (2013) The East Anatolian Fault: geometry, segmentation and jog characteristics. In: Robertson AHF, Parlak O, Ünlügenç UC (ed) *Geological Development of Anatolia and the Easternmost Mediterranean Region*, Geological Society of London Special Publications, 495–529. <https://doi.org/10.1144/SP372.14>
- Duran İ, Sözbilir H, Eski S, Softa M, Uytun H et al (2021) Paleoseismic history of the Manisa fault zone, Western Anatolia. *Turk J Earth Sci* 30(SI-1):806–832
- Emre Ö, Barka A (2000) Gediz Grabeni Ege denizi arasının (İzmir yöresi) aktif fayları. In: *Batı Anadolu Depremselliği Sempozyumu (BADSEM 2000)*, p 131–132, İzmir, Turkey (in Turkish)
- Emre Ö, Duman TY, Özalp S, Şaroğlu F, Olgun Ş et al (2018) Active fault database of Turkey. *Bull Earthq Eng* 16(8):3229–3275. <https://doi.org/10.1007/s10518-016-0041-2>
- Emre Ö, Özalp S (2011) 1:250,000 Ölçekli Türkiye Diri Fay Haritası Serisi, Urla (NJ 35-6) Paftası, Seri No:5. Ankara: Maden Tetkik ve Arama Genel Müdürlüğü (in Turkish)
- Emre Ö, Özalp S, Doğan A, Özaksoy V, Yıldırım C et al. (2005) İzmir yakın çevresinin diri fayları ve deprem potansiyelleri - Rapor No: 10754. Ankara: Maden Tetkik ve Arama Genel Müdürlüğü (in Turkish)

- Emre Ö, Özalp S, Duman TY (2011) 1:250.000 Ölçekli Türkiye Diri Fay Haritası Serisi, İzmir (NJ 35-7) Paftası, Seri No:6. Ankara: Maden Tetkik ve Arama Genel Müdürlüğü (in Turkish)
- Erdoğan B (1990) Stratigraphic features and tectonic evolution of the İzmir-Ankara Zone located between İzmir and Seferihisar. *Turk Assoc Petrol Geol (TPJD) Bull* 2:1–20
- Ergin K, Güçlü U, Uz Z (1967) Türkiye ve Civarının Deprem Kataloğu (Milattan Sonra 11 Yılından 1964 Sonuna Kadar), 24. İTÜ Maden Fakültesi Arz Fiziği Enstitüsü Yayınları, İstanbul (in Turkish)
- Eşder T (1988) Gümüldür-Cumaovası (İzmir) alanının jeolojisi ve jeotermal enerji olanaklarının araştırılması. PhD, İstanbul University, İstanbul, Turkey (in Turkish)
- Eşder T, Şimşek Ş (1975) Geology of İzmir (Seferihisar) geothermal area, Western Anatolia of Turkey: determination of reservoirs by means of gradient drilling. In: *Proceedings of 2nd UN. Symposium*, pp 349–361
- Eyübagil EE, Solak Hİ, Kavak US, Tiryakioğlu İ, Sözbilir H et al (2021) Present-day strike-slip deformation within the southern part of İzmir Balıkesir Transfer Zone based on GNSS data and implications for seismic hazard assessment, western Anatolia. *Turk J Earth Sci* 30(2):143–160. <https://doi.org/10.3906/yer-2005-26>
- Fan X, Juang CH, Wasowski J, Huang R, Xu Q, Scaringi G, van Westen CJ, Havenith HB (2018) What we have learned from the 2008 Wenchuan Earthquake and its aftermath: a decade of research and challenges. *Eng Geol* 241:25–32
- Fattahi M, Nazari H, Bateman MD, Meyer B, Se'brrier M, et al (2010) Refining the OSL age of the last earthquake on the Dhesir fault, Central Iran. *Quat Geochronol* 5(2–3):286–292. <https://doi.org/10.1016/j.quageo.2009.04.005>
- Fattahi M, Walker R, Hollingsworth J, Bahroudi A, Nazari H et al (2006) Holocene slip-rate on the Sabzevar thrust fault, NE Iran, determined using optically stimulated luminescence (OSL). *Earth Planet Sci Lett* 245(3–4):673–684
- Galbraith RF (1990) The radial plot: graphical assessment of spread in ages. *Int J Radiat Appl Instrum Part D Nucl Tracks Radiat Measur* 17(3):207–214
- Galbraith RF, Roberts RG, Laslett GM, Yoshida H, Olley JM (1999) Optical dating of single and multiple grains of quartz from Jinmium rock shelter, northern Australia: Part I, experimental design and statistical models. *Archaeometry* 41(2):339–364
- Galbraith RF, Roberts RG, Yoshida H (2005) Error variation in OSL palaeodose estimates from singles aliquots of quartz: a factorial experiment. *Radiat Meas* 39:289–307
- Galli P, Galadini F, Pantosti D (2008) Twenty years of paleoseismology in Italy. *Earth Sci Rev* 88(1–2):89–117
- Genç CŞ, Altunkaynak Ş, Karacık Z, Yazman M, Yılmaz Y (2001) The Çubukludağ graben, south of İzmir: its tectonic significance in the Neogene geological evolution of the western Anatolia. *Geodin Acta* 14(1–3):45–55
- Göktaş F (2019) Çubukludağ Havzasındaki Neojen Tortullaşması ve Volkanizmasının Stratigrafisi. *Batu Anadolu Türkiye Jeoloji Bülteni* 62(1):63–98
- Göktaş F, Çakmakoğlu A (2018) 1:100.000 ölçekli Türkiye Jeoloji Haritaları Serisi, Urla-L16 Paftası, No: 258, Maden Tetkik ve Arama Genel Müdürlüğü, Ankara
- Guidoboni E, Comastri A, Triana G (1994) Catalogue of Ancient Earthquakes in the Mediterranean Area up to the 10th Century. *Istituto Nazionale di Geofisica*, p 504, ISBN 88-85213-06-5
- Gürboğa Ş, Gökçe O (2019) Palaeoseismology catalog of Pre-2012 trench studies on the active faults in Turkey. *Bull Min Res Explor* 159(159):63–87
- Gürçay S (2014) Sığacık körfezi ve çevresinin deniz altı aktif tektoniğinin yüksek çözünürlüklü sismik yöntemler uygulanarak araştırılması. PhD, Dokuz Eylül University, İzmir, Turkey (in Turkish)
- Ikeda Y, Herece E, Sugai T, Işıkara AM (1991) Postglacial crustal deformation associated with slip on the western part of the North Anatolian Fault Zone in the Iznik Lake Basin, Turkey. *Bull Dep Geogr* 23:13–23
- ISC (International Seismological center) (2023) Recent Earthquakes in Turkey [online]. Website <http://www.isc.ac.uk/> [accessed 12 Jan 2023]
- Jayangondaperumal R, Kumahara Y, Thakur VC, Kumar A, Srivastava P et al (2017) Great earthquake surface ruptures along backthrust of the Janauri anticline, NW Himalaya. *J Asian Earth Sci* 133:89–101
- Jayangondaperumal R, Thakur VC, Jovivek V, Rao PS, Gupta AK (2018) Active tectonics of Kumaun and Garhwal Himalaya, Springer Natural Hazards, 150 pp. ISBN 978-981-10-8242-9.
- Jolivet L, Faccenna C, Huet B, Labrousse L, Le Pourhiet L et al (2013) Aegean tectonics: strain localisation, slab tearing and trench retreat. *Tectonophysics* 597:1–33
- Karabacak V (2016) Seismic damage in the Lagina sacred area on the Mugla Fault: a key point for the understanding of the obliquely situated faults of western Anatolia. *J Seismolog* 20(1):277–289

- Karacık Z, Genç ŞC (2013) Volcano-stratigraphy of the extension-related silicic volcanism of the Çubukludağ Graben, western Turkey: an example of generation of pyroclastic density currents. *Geol Mag* 151(3):492–516
- Kaya O (1979) Ortadoğu Ege çöküntüsünün (Neojen) stratigrafisi ve tektoniği (Neogene stratigraphy and tectonics of the MiddleEast Aegean depression). *Bull Geol Soc Turk* 22:35–58
- Kaya O (1981) Miocene reference section for the coastal parts of West Anatolia. *Newslett Stratigr* 10:164–191
- Kempf P, Moernaut J (2021) Age uncertainty in recurrence analysis of paleoseismic records. *J Geophys Res: Solid Earth*. <https://doi.org/10.1029/2021JB021996>
- Kırkan E, Akyüz HS, Basmenji M, Dikbaş A, Zabcı C et al (2023) Earthquake history of the Milas Fault: an active dextral fault in an extensional province (SW Anatolia, Turkey). *Nat Hazards*. <https://doi.org/10.1007/s11069-022-05733-w>
- Kırkan E, Akyüz HS, Basmenji M, Zabcı C, Dikbaş A et al. (2019) Tectonic and palaeoseismology analysis of active deformation along the Milas Fault (Muğla, SW Turkey): earthquake history and seismicity. In: 23rd Active Tectonics Research Group Meeting; İstanbul, Turkey. pp 98
- Kürçer A, Gökten YE (2014) Neotectonic-period characteristics, seismicity, geometry and segmentation of the Tuz Gölü fault zone. *Bull Min Res Explor* 149(149):19–68
- Lee J, Spencer JQ, Owen LA (2001) Holocene slip rates along the Owens Valley fault, California: implications for the recent evolution of the Eastern California Shear Zone. *Geology* 29(9):819–822. <https://doi.org/10.1029/2006GL026734>
- Lykousis V, Anagnostou C, Pavlakis P, Rousakis G, Alexandri M (1995) Quaternary sedimentary history and neotectonic evolution of the eastern part of Central Aegean Sea. *Greece Marine Geol* 128(1–2):59–71
- Mackenzie D, Elliott JR, Altunel E, Walker RT, Kurban YC, Schwenninger JL, Parsons B (2016) Seismotectonics and rupture process of the MW 7.1 2011 Van reverse-faulting earthquake, eastern Turkey, and implications for hazard in regions of distributed shortening. *Geophys J Int* 206(1):501–524
- Mahan SA, Rittenour TM, Nelson MS, Ataee N, Brown N, DeWitt R, Durcan J, Evans M, Feathers J, Frouin M, Guérin G, Heydari M, Huot S, Jain M, Keen-Zebert A, Li B, López GI, Neudorf C, Porat N, Rodrigues K, Sawakuchi AO, Spencer JQG, Thomsen K (2022) Guide for interpreting and reporting luminescence dating results. *GSA Bull* 135:1480–1502. <https://doi.org/10.1130/B36404.1>
- McCalpin JP (2009) Application of paleoseismic data to seismic hazard assessment and neotectonic research. *Int Geophys* 95:1–106
- Meng J, Sinoplu O, Zhou Z, Tokay B, Kusky T et al (2021) Greece and Turkey Shaken by African tectonic retreat. *Sci Rep* 11:6486
- Mozafari N, Özkaymak Ç, Sümer Ö, Tikhomirov D, Uzel B et al (2022) Seismic history of western Anatolia during the last 16 kyr determined by cosmogenic ³⁶Cl dating. *Swiss J Geosci* 115:5
- Mozafari N, Özkaymak Ç, Tikhomirov D, Ivy-Ochs S, Alfimov V et al (2021) Seismic activity of the Manisa fault zone in Western Turkey constrained by cosmogenic ³⁶Cl dating. *Geosciences* 11:451
- Murray AS, Wintle AG (2000) Luminescence dating of Quartz using an improved single Aliquot regenerative-dose protocol. *Radiat Meas* 32:57–73
- Nas M, Lyubushin A, Softa M, Bayrak Y (2020) Comparative PGA-driven probabilistic seismic hazard assessment (PSHA) of Turkey with a Bayesian perspective. *J Seismolog* 24:1109–1129
- Nyst M, Thatcher W (2004) New constraints on the active tectonic deformation of the Aegean. *J Geophys Res Solid Earth*. <https://doi.org/10.1029/2003JB002830>
- Ocakoğlu N, Demirbağ E, Kuşçu İ (2004) Neotectonic structures in the area offshore of Alaçatı, Doğanbey and Kuşadası (western Turkey): evidence of strike-slip faulting in the Aegean extensional province. *Tectonophysics* 391:67–83
- Ocakoğlu N, Demirbağ E, Kuşçu İ (2005) Neotectonic structures in İzmir Gulf and surrounding regions (western Turkey): evidences of strike-slip faulting with compression in the Aegean extensional regime. *Mar Geol* 219:155–171
- Okay AI, İşintek İ, Altuner D, Özkan-Altuner S, Okay N (2012) An olistostrome–mélange belt formed along a suture: Bornova Flysch zone, western Turkey. *Tectonophysics* 568:282–295
- Özer S, İrtəm O (1982) Işıklar-Altındağ (Bornova-İzmir) alanı Üst Kretase kireçtaşlarının jeolojik konumu, stratigrafisi ve fasiyesi özellikleri. *Türkiye Jeoloji Kurumu Bülteni* 25:41–47
- Özkaymak Ç, Sözbilir H (2008) Stratigraphic and structural evidence for fault reactivation: the active Manisa Fault Zone, Western Anatolia. *Turk J Earth Sci* 17:615–635
- Özkaymak Ç, Sözbilir H (2012) Tectonic geomorphology of the Spildağı High Ranges, Western Anatolia. *Geomorphology* 173–174:128–140


- Özkaymak Ç, Sözbilir H, Uzel B (2013) Neogene-quaternary evolution of the Manisa Basin: Evidence for variation in the stress pattern of the İzmir-Balıkesir Transfer Zone, Western Anatolia. *J Geodyn* 65:117–135
- Özkaymak Ç, Sözbilir H, Uzel B, Akyüz HS (2011) Geological and palaeoseismological evidence for late Pleistocene-Holocene activity on the Manisa fault zone, western Anatolia. *Turk J Earth Sci* 20(4):449–474. <https://doi.org/10.3906/yer-0906-18>
- Pavlidis S, Tsapanos T, Zouros N, Sboras S, Koravos G et al (2009) Using active fault data for assessing seismic hazard: a case study from NE Aegean Sea, Greece. In: Earthquake geotechnical engineering satellite conference XVIIIth international conference on soil mechanics & geotechnical engineering, Vol 10, p 2009
- Prentice CS, Kendrick K, Berryman K, Bayasgalan A, Ritz JF, Spencer JQ (2002) Prehistoric ruptures of the Gurvan Bulag fault, Gobi Altay, Mongolia. *J Geophys Res* 107(B12):2321. <https://doi.org/10.1029/2001JB000803>
- Preusser F, Degering D, Fuchs M, Hilgers A, Kadereit A et al (2008) Luminescence dating: basics, methods and applications. *E&G Quat Sci J* 57(1/2):95–149. <https://doi.org/10.3285/eg.57.1-2.5>
- Priyanka RS, Jayangondaperumal R, Pandey A, Mishra RL, Singh I et al (2017) Primary surface rupture of the 1950 Tibet-Assam great earthquake along the eastern Himalayan front, India. *Sci Rep* 7(1):1–12. <https://doi.org/10.1038/s41598-017-05644-y>
- Ramsey CB (1995) Radiocarbon calibration and analysis of stratigraphy: the OxCal program. *Radiocarbon* 37(2):425–430
- Ramsey CB (2001) Development of the radiocarbon calibration program. *Radiocarbon* 43(2A):355–363
- Ramsey CB (2008) Deposition models for chronological records. *Quat Sci Rev* 27(1–2):42–60. <https://doi.org/10.1016/j.quascirev.2007.01.019>
- Ramsey CB (2009) Bayesian analysis of radiocarbon dates. *Radiocarbon* 51(1):337–360
- Reimer PJ, Baillie MG, Bard E, Bayliss A, Beck JW et al (2009) IntCal09 and Marine09 radiocarbon age calibration curves, 0–50,000 years cal BP. *Radiocarbon* 51(4):1111–1150. <https://doi.org/10.1017/S0033822200034202>
- Reilinger R, McClusky S, Vernant P, Lawrence S, Ergintav S et al (2006) GPS constraints on continental deformation in the Africa-Arabia-Eurasia continental collision zone and implications for the dynamics of plate interactions. *J Geophys Res: Solid Earth*. <https://doi.org/10.1029/2005JB004051>
- Reilinger R, McClusky S, Paradissis D, Ergintav S, Vernant P (2010) Geodetic constraints on the tectonic evolution of the Aegean region and strain accumulation along the Hellenic subduction zone. *Tectonophysics* 488(1–4):22–30
- Rhodes EJ (2011) Optically stimulated luminescence dating of sediments over the past 200,000 years. *Annu Rev Earth Planet Sci* 39:461–488
- Rittase WM, Kirby E, McDonald E, Walker JD, Gosse J, Spencer JQG, Herrs AJ (2014) Temporal variations in Holocene slip rate along the central Garlock fault, Pilot Knob Valley, California. *Lithosphere* 6(1):48–58. <https://doi.org/10.1130/L286.1>
- Rockwell TK, Keller EA, Johnson DL (1984) Tectonic geomorphology of alluvial fans and mountain fronts near Ventura, California. In: Morisawa, M (ed). *Tectonic Geomorphology*. Proceedings of the 15th Annual Geomorphology Symposium. 1st ed. Boston, MA: Allen and Unwin Publishers, pp 183–207
- Sarı B (2013) Late Maastrichtian-late Palaeocene planktic foraminiferal biostratigraphy of the matrix of the Bornova Flysch Zone around Bornova (İzmir, western Anatolia, Turkey). *Turk J Earth Sci* 22(1):143–171
- Scordilis E, Kiratzi A, Panagiotopoulos D (1994) A study of the earthquake of Nov 6, 1992 in Izmir (Turkey). *Bull Geol Soc. Greece* XXX/5, 243–249
- Silva PG, Goy JL, Zazo C, Bardaji T (2003) Fault-generated mountain fronts in southeast Spain: geomorphologic assessment of tectonic and seismic activity. *Geomorphology* 50(1–3):203–225
- Slemmons DB, Depolo CM (1986) Evaluation of active faulting and associated hazards. *Active Tecton* 1986:45–62
- Softa M, Spencer JQ, Sözbilir H, Huot S, Emre T (2021) Luminescence dating of Quaternary marine terraces from the coastal part of Eastern Black Sea and their tectonic implications for the Eastern Pontides, Turkey. *Turki J Earth Sci*. <https://doi.org/10.3906/yer-2005-21>
- Softa M, Sahiner E, Sözbilir H, Spencer JQG, Utku M, Büyüktopçu, F (2023) The first application of the luminescence surface exposure dating method on active fault scarps in the Western Anatolia extensional province: the Manisa Fault as an example. *Turki J Earth Sci* 32(2):163–180. <https://doi.org/10.55730/1300-0985.1836>
- Softa M, Utku M (2022) Paleosismoloji Çalışmalarında Kollüvyal Çökellerdeki Su İçeriğinin Lüminesans Tarihlendirmeye Etkisinin Değerlendirilmesi; Soma-Kırkağaç Fayı'ndan Bir Örnek. *Afyon Kocatepe Üniversitesi Fen Ve Mühendislik Bilimleri Dergisi* 22(2):417–430

- Soysal H, Sipahioğlu S, Kolçak D, Altınok Y (1981) Türkiye ve Çevresinin Tarihsel Deprem Katalogu (M.Ö. 2100-M.S.1900), TÜBİTAK, Proje No: TBAG-341 (in Turkish)
- Sözbilir H, İnci U, Erkül F, Sümer Ö (2003) An active intermittent transfer zone accomodating N-S extension in Western Anatolia and its relation to the Nort Anatolian Fault system. In: International Workshop on the North Anatolian, East Anatolian and Dead Sea Fault Systems: Recent Progress in Tectonics and Palaeoseismology and Field Training Course in Palaeoseismology, Ankara, Turkey, p 8
- Sözbilir H, Özkaymak Ç, Sümer Ö, Softa M, Spencer JQG, Eski S, Tepe Ç, Şengöçmen Geçkin B, Öncü U, Şahiner E, Yüksel M, Meriç N, Topaksu M (2021) Active tectonics and paleoseismology of seismic sources located on land in the vicinity of the city of İzmir, western Anatolia, Turkey. International Workshop on Active Tectonics and Seismicity of the Aegean Region with Special Emphasis on the Samos Earthquake Struck on 30 October 2020 (ASASE2021)/ 20–21 May 2021 – TURKEY, Turkish Journal of Earth Sciences, 30: MA-6.
- Sözbilir H, Sarı B, Uzel B, Sümer Ö, Akkiraz S (2011) Tectonic implications of transtensional supra-detachment basin development in an extension-parallel transfer zone: the Kocaçay Basin, western Anatolia. *Turk Basın Res* 23(4):423–448
- Spencer JQG, Sanderson DCW, Deckers K, Sommerville AA (2003) Assessing mixed dose distributions in young sediments identified using small aliquots and a simple two-step SAR procedure: the F-statistic as a diagnostic tool. *Radiat Meas* 37(4–5):425–431. [https://doi.org/10.1016/S1350-4487\(03\)00064-7](https://doi.org/10.1016/S1350-4487(03)00064-7)
- Spencer JQG, Robinson RA (2008) Dating intramontane alluvial deposits from NW Argentina using luminescence techniques: problems and potential. *Geomorphology* 93(1–2):144–155. <https://doi.org/10.1016/j.geomorph.2006.12.021>
- Spencer JQG, Huot S, Archer AW, Caldas MM (2019) Testing luminescence dating methods for small samples from very young fluvial deposits. *Methods Protoc* 2(4):90. <https://doi.org/10.3390/mps2040090>
- Stahl T, Quigley MC, McGill A, Bebbington MS (2016) Modeling earthquake moment magnitudes on imbricate reverse faults from palaeoseismic data: fox peak and forest creek faults, South Island, New Zealand. *Bull Seismol Soc Am* 106(5):2345–2363
- Stucchi M, Rovida A, Gomez Capera AA, Alexandre P, Camelbeeck T et al (2012) The SHARE European earthquake catalogue (SHEEC) 1000–1899. *J Seismolog*. <https://doi.org/10.1007/s10950-012-9335-2>
- Şaroğlu F, Emre Ö, Boray A (1987) Türkiye'nin diri fayları ve depremsellikleri. Ankara: Maden Tetkik ve Arama Genel Müdürlüğü Jeoloji Etüdüleri Dairesi Başkanlığı (in Turkish)
- Şaroğlu F, Emre Ö, Kuşçu İ (1992) Türkiye Diri Fay Haritası, 1:2,000,000 ölçekli. Ankara: Maden Tetkik ve Arama Genel Müdürlüğü (in Turkish)
- Şengöçmen Geçkin B, Sözbilir H, Özkaymak Ç, Softa M, Spencer JQG et al (2022) Evidence of surface rupture associated with historical earthquakes on the Gülbağçe Fault Zone (İzmir, Turkey) and its application for determination of the surface fault-rupture hazard zone. *Nat Hazards*. <https://doi.org/10.1007/s11069-022-05467-9>
- Şengör AMC, Görür N, Şaroğlu F (1985) Strike-slip faulting and related basin formation in zones of tectonic escape: Turkey as a case study. In: Biddle K, Christie-Blick N (Eds), Strike-slip deformation, basin formation and sedimentation. Society of Economic Paleontologists and Mineralogists. Special Publications 37: 227–264
- Şengör AMC, Tüysüz O, Imren C, Sakiç M, Eyidoğan H et al (2005) The North Anatolian fault: a new look. *Annu Rev Earth Planet Sci* 33:37–112
- Tan O, Tapırdamaz MC, Yörük A (2008) The Earthquakes catalogues for Turkey. *Turk J Earth Sci* 17:405–418
- Tan O, Taymaz T (2001) Source parameters of November 6, 1992 Doğanbey (İzmir) earthquake (Mw = 6.0) obtained from inversion of teleseismic body-waveforms. In: Proceedings of 4th International Turkish Geology Symposium: Work in Progress on the Geology of Turkey and its Surroundings, Çukurova University Publications, Adana, Turkey, p 171
- Tan O, Taymaz T (2003) Seismotectonics of Karaburun Peninsula and Kuşadası Gulf: source parameters of April 2, 1996 Kuşadası Gulf and April 10, 2003 Seferihisar (İzmir) earthquakes. In: International Workshop on the North Anatolian, East Anatolian and Dead Sea Fault Systems: Recent Progress in Tectonics and Palaeoseismology and Field Training Course in Palaeoseismology, Middle East Technical University (METU), Ankara, Turkey, p 147
- Tatar O, Sözbilir H, Koçbulut F, Bozkurt E, Aksoy E et al (2020) Surface deformations of 24 January 2020 Sivrice (Elazığ)–Doğanyol (Malatya) earthquake (Mw= 6.8) along the Pütürge segment of the East Anatolian Fault Zone and its comparison with Turkey's 100-year-surface ruptures. *Mediterr Geosci Rev* 2(3):385–410

- Tepe Ç, Sözbilir H, Eski S, Sümer Ö, Özkaymak Ç (2021) Updated historical earthquake catalog of İzmir region (western Anatolia) and its importance for the determination of seismogenic source. *Turk J Earth Sci* 30:779–805
- Tsodoulos IM, Stamoulis K, Caputo R, Koukouvelas I, Chatzipetros A et al (2016) Middle-Late Holocene earthquake history of the Gyroni Fault, Central Greece: insight from optically stimulated luminescence (OSL) dating and palaeoseismology. *Tectonophysics* 687:14–27. <https://doi.org/10.1016/j.tecto.2016.08.015>
- Türkelli H, Kalafat D, Gündoğdu O (1995) November, 6, 1992 İzmir (Doğanbeyli) earthquake, field observations and focal mechanism solutions. *Geophysics* 9(10):343–348 (**in Turkish**)
- Uzel B, Langereis CG, Kaymakci N, Sözbilir H, Özkaymak Ç, Özkaptan M (2015) Paleomagnetic evidence for an inverse rotation history of Western Anatolia during the exhumation of Menderes core complex. *Earth Planet Sci Lett* 414:108–125
- Uzel B, Sözbilir H (2008) A First record of strike-slip basin in western Anatolia and its tectonic implication: the Cumaovası basin as an example. *Turk J Earth Sci* 17:559–591
- Uzel B, Sözbilir H, Özkaymak Ç, Kaymakci N, Langereis CG (2013) Structural evidence for strike-slip deformation in the İzmir-Balıkesir transfer zone and consequences for late Cenozoic evolution of western Anatolia (Turkey). *J Geodyn* 65:94–116. <https://doi.org/10.1016/j.jog.2012.06.009>
- Uzelli T, Bilgiç E, Öztürk B, Baba A, Sözbilir H et al (2021) Effects of seismic activity on groundwater level and geothermal systems in İzmir, Western Anatolia, Turkey: the case study from October 30, 2020 Samos Earthquake. *Turk J Earth Sci* 30(8):758–778
- Wallinga J, Cunningham AC (2014) Luminescence Dating, Uncertainties, and Age Range. In: Rink W, Thompson J (eds) *Encyclopedia of Scientific Dating Methods*. Springer, Dordrecht
- Wells DL, Coppersmith KJ (1994) New empirical relationships among magnitude, rupture length, rupture width, rupture area and surface displacement. *Bull Seismol Soc Am* 84(4):974–1002
- Westaway R (1994) Present-day kinematics of the Middle East and eastern Mediterranean. *J Geophys Res: Solid Earth* 99(B6):12071–12090

Publisher's Note Springer Nature remains neutral with regard to jurisdictional claims in published maps and institutional affiliations.

Authors and Affiliations

Umut Öncü¹  · Hasan Sözbilir^{2,3}  · Çağlar Özkaymak^{4,5}  · Mustafa Softa^{2,3}  ·
Ökmen Sümer²  · Semih Eski^{1,2}  · Joel Q. G. Spencer⁶  · Eren Şahiner⁷  ·
Mehmet Yüksel⁸  · Niyazi Meriç⁷  · Mustafa Topaksu⁸ 

✉ Umut Öncü
umut.oncu@ogr.deu.edu.tr

¹ Department of Geological Engineering, The Graduate of Natural and Applied Sciences, Dokuz Eylül University, 35390 Buca, İzmir, Turkey

² Department of Geological Engineering, Faculty of Engineering, Dokuz Eylül University, 35390 Buca, İzmir, Turkey

³ Earthquake Research and Application Center of Dokuz, Eylül University, 35390 Buca, İzmir, Turkey

⁴ Department of Geological Engineering, Faculty of Engineering, Afyon Kocatepe University, 03200 Afyonkarahisar, Turkey

⁵ Earthquake Implementation and Research Center of Afyon Kocatepe University, 03200 Afyonkarahisar, Turkey

⁶ Department of Geology, Kansas State University, Manhattan, KS 66506, USA

⁷ Institute of Nuclear Sciences, Ankara University, 06100 Beşevler, Ankara, Turkey

⁸ Department of Physics, Faculty of Arts-Sciences, Çukurova University, 01250 Adana, Turkey